Measurement of multi-jet cross sections in proton-proton collisions at a 7 TeV center-of-mass energy

Aad, G.; et al., [Unknown]; Bentvelsen, S.; Colijn, A.P.; de Jong, P.; de Nooij, L.; Doxiadis, A.D.; Ferrari, P.; Garitaonandia, H.; Geerts, D.A.A.; Gosselink, M.; Kayl, M.S.; Koffeman, E.; Lee, H.; Linde, F.; Mechnich, J.; Mussche, I.; Ottersbach, J.P.; Tsiakiris, M.; van der Kraaij, E.; van der Leeuw, R.; van Kesteren, Z.; van Vulpen, I.; Vermeulen, J.C.; Vreeswijk, M.

DOI
10.1140/epjc/s10052-011-1763-6

Publication date
2011

Document Version
Final published version

Published in
European Physical Journal C

Eur. Phys. J. C (2011) 71:1763
DOI 10.1140/epjc/s10052-011-1763-6

THE EUROPEAN PHYSICAL JOURNAL C

Regular Article - Experimental Physics

Measurement of multi-jet cross sections in proton–proton collisions at a 7 TeV center-of-mass energy

The ATLAS Collaboration*
CERN, 1211 Geneva 23, Switzerland

Received: 11 July 2011 / Revised: 9 September 2011 / Published online: 15 November 2011

Abstract Inclusive multi-jet production is studied in proton–proton collisions at a center-of-mass energy of 7 TeV, using the ATLAS detector. The data sample corresponds to an integrated luminosity of 2.4 pb^{-1}. Results on multi-jet cross sections are presented and compared to both leading-order plus parton-shower Monte Carlo predictions and to next-to-leading-order QCD calculations.

1 Introduction

At hadron colliders, events containing multiple jets in the final state are plentiful and provide a fertile testing ground for the theory of the strong interaction, quantum chromodynamics (QCD). At high transverse momentum (p_{T}), the production of jets is modeled by QCD as the hard scattering of partons and the subsequent parton showering, followed by a hadronization process. Within this framework, the jet energy is related to the energy of partons produced in hadron collisions. Consequently, the study of energy distributions for multi-jet events provides a fundamental and direct test of QCD at hadron colliders.

In addition to their role in testing QCD, multi-jet events are often an important background in searches for new particles and new interactions at high energies. In particular, systematic uncertainties that contribute to multi-jet cross section measurements can carry over into search analyses. Even though the impact of multi-jets on such analyses will vary according to the specific data selection criteria, a study of multi-jet events serves as an important cross check of models used to estimate backgrounds originating from jets.

Measurements of multi-jet cross sections at the Tevatron have been performed by the CDF [1, 2] and D0 [3, 4] collaborations in proton–antiproton collisions at 1.8 TeV center-of-mass energy. The CMS collaboration has recently released measurements of the three-jet to two-jet cross sections at a 7 TeV center-of-mass energy [5]. In this paper, a first study is performed of multi-jet events from proton–proton collisions at 7 TeV center-of-mass energy using the ATLAS detector at the Large Hadron Collider (LHC) at CERN. The data sample used for the analysis was collected from April until August 2010 and represents a total integrated luminosity of 2.4 pb^{-1}. Approximately half a million events with at least two jets in the final state are selected using this data sample.

Two primary motivations for the multi-jet study in this paper are to evaluate how robust leading-order perturbative QCD (LO pQCD) calculations are in representing the high jet multiplicity events, and to test next-to-leading-order perturbative QCD (NLO pQCD) calculations. For the leading-order comparisons, events with up to six jets in the final state are studied, and for the next-to-leading-order perturbative QCD study, the focus is on three-jet events and their comparison to two-jet events. At present, there is no four-jet NLO pQCD calculation available.

The paper is organized as follows. Section 2 presents a description of the ATLAS detector. Section 3 discusses the cross sections and kinematics. In Sect. 4, theoretical calculations, to which the measurements are compared, are described. Sections 5 and 6 discuss the event selection and data corrections. The main uncertainty coming from the jet energy scale is discussed in Sect. 7, followed by the results and conclusions.

2 The ATLAS detector

The ATLAS experiment consists of an approximately 45-meter long, 25-meter diameter cylindrically shaped detector centered on the proton–proton interaction point. A detailed description of the ATLAS experiment can be found elsewhere [6]. High-energy particles produced in collisions initially pass through an inner tracking system embedded in a

* e-mail: atlas.publications@cern.ch

2 T solenoidal magnetic field. The field is located in a region of diameter 2.3 meters and 7 meters long also centered at the interaction point. The design of this tracking system allows the measurement of charged particle kinematics within the pseudorapidity[1] range of $|\eta| < 2.5$. Precision tracking using the pixel detector with a space point resolution as small as 10 microns by 70 microns (in the beam direction) begins at a radial distance of 5 cm from the interaction point [7]. The identification of the vertex from which the jet originates, performed with the inner tracker, is of interest in the study of multi-jet events.

Just outside the inner tracker system are liquid argon and scintillating tile calorimeters used for the measurement of particle energies. A liquid-argon/lead electromagnetic calorimeter covers the pseudorapidity range of $|\eta| < 3.2$. This calorimeter is complemented by hadronic calorimeters, built using scintillating tiles and iron for $|\eta| < 1.7$ and liquid argon and copper in the end-cap ($1.5 < |\eta| < 3.2$). Forward calorimeters extend the coverage to $|\eta| = 4.9$. The calorimeters are the primary detectors used to reconstruct the jet energy in this analysis and allow the reconstruction of the jet p_T with a fractional resolution of better than 0.10 for jets of $p_T = 60$ GeV and 0.05 for jets of $p_T = 1$ TeV.

Outside the calorimeters is a toroidal magnetic field that extends to the edge of the detector. Additional tracking detectors designed for measuring muon kinematics are placed within this magnetic field. The impact of muons in the analysis presented in this paper is negligible.

The ATLAS trigger system employs three trigger levels, of which only the hardware-based first level trigger is used in this analysis. Events are selected using the calorimeter based jet trigger. The first level jet trigger [8] uses coarse detector information to identify areas in the calorimeter where energy deposits above a certain threshold occur. A simplified jet finding algorithm based on a sliding window of size $\Delta\phi \times \Delta\eta = 0.8 \times 0.8$ is used to identify these areas. This algorithm uses coarse calorimeter towers with a granularity of $\Delta\phi \times \Delta\eta = 0.2 \times 0.2$ as inputs.

3 Cross section definitions and kinematics

In this analysis, the anti-k_t algorithm [9, 10], with jet constituents combined according to their four-momenta, is used to identify jets. For high multiplicity studies, which includes events with up to six jets, the resolution parameter in the jet reconstruction is fixed to $R = 0.4$ to contend with the limited phase space and to reduce the impact of the underlying event in the jet energy determination. For testing NLO pQCD calculations, where the study focuses on three-jet events, a resolution parameter of $R = 0.6$ is preferred, since a larger value of R is found to be less sensitive to theoretical scale uncertainties. The anti-k_t algorithm was chosen for a variety of reasons. It can be implemented in the NLO pQCD calculation, is infra-red and collinear safe to all orders, and reconstructs jets with a simple geometrical shape.

Jet measurements are corrected for all experimental effects such that they can be compared to particle-level predictions. At the particle level, jets are built using all final-state particles with a proper lifetime longer than 10 ps. These corrections are described in Sect. 6. The NLO pQCD calculation is not interfaced to a Monte Carlo simulation with hadronization and other non-perturbative effects. The correction for non-perturbative effects applied to the NLO pQCD calculation is described in Sect. 4.

Cross sections are calculated in bins of inclusive jet multiplicity, meaning that an event is counted in a jet multiplicity bin if it contains a number of jets that is equal to or greater than that multiplicity. For example, an event with three reconstructed jets will be counted both in the two-jet and three-jet multiplicity bins. Inclusive multiplicity bins are used because they are stable in the pQCD fixed-order calculation, unlike exclusive bins. Only jets with $p_T > 60$ GeV and $|y| < 2.8$ are counted in the analysis. These cuts are chosen to ensure that the jets are reconstructed with high efficiency. The leading jet is further required to have $p_T >$ 80 GeV to stabilize the NLO pQCD calculations in the dijet case [11].

4 Theoretical predictions

Measurements are compared to pQCD calculations at leading order and next-to-leading order.

Many different effects are included in leading-order Monte Carlo simulations of jets at the LHC. These include the modeling of the underlying event and hadronization, which can affect the cross section calculation through their impact on the jet kinematics [12]. Effects arising from differences between the matrix-element plus parton-shower (ME+PS) calculation (with up to $2 \to n$ matrix-element scattering diagrams) and the parton-shower calculation alone (with only $2 \to 2$ matrix-element scattering diagrams) also need to be understood. These topics are not easily separable, since tuning of some of the effects (such as the underlying event) to data is needed, and the tuning process fixes other inputs in the Monte Carlo simulation,

[1] ATLAS uses a right-handed coordinate system with its origin at the nominal interaction point (IP) in the center of the detector and the z-axis along the beam pipe. The x-axis points from the IP to the center of the LHC ring, and the y axis points upward. Cylindrical coordinates (r, ϕ) are used in the transverse plane, ϕ being the azimuthal angle around the beam pipe. The pseudorapidity is defined in terms of the polar angle θ as $\eta = -\ln\tan(\theta/2)$. The rapidity is defined as $y = 0.5 \times \ln[(E + p_z)/(E - p_z)]$, where E denotes the energy and p_z is the component of the momentum along the beam direction. For massless objects, the rapidity and pseudorapidity are equivalent.

such as the proton parton distribution functions (PDF), the parton-shower model, and the hadronization model. The inability to separate out some effects makes it difficult to obtain a full estimate of the theoretical uncertainty associated with the leading-order Monte Carlo predictions. Furthermore, leading-order Monte Carlo predictions are affected by large normalization uncertainties.

In this study, the goal is to test the performance of the different leading-order Monte Carlo simulations, so that they can be used to estimate multi-jet backgrounds for new particle searches, not to discern whether deviations with respect to QCD are present in the data. The latter goal is best achieved by comparing with NLO pQCD calculations (discussed later in this section). For these reasons, the leading-order Monte Carlo predictions are all normalized to the measured inclusive two-jet cross section and then used for shape comparisons. No attempt is made to assign a theoretical uncertainty to these leading-order predictions. Instead, numerous different Monte Carlo simulations and currently available tunes have been studied in order to investigate the impact of each of these effects on the measurements. Only a representative subset is shown in the results, even though conclusions are drawn on the basis of all simulations studied.

For the leading-order analysis, ALPGEN [13] is used to generate events with up to six partons in the final state using the leading-order set of proton PDFs CTEQ6L1 [14]. A factorization and renormalization scale, Q, that varies from event to event is used in the event generation, where $Q^2 = \sum p_{\mathrm{T}}^2$. The sum runs over all final state partons. ALPGEN is interfaced to PYTHIA 6.421 [15, 16] and, alternatively, to HERWIG/JIMMY [17–20] to sum leading logarithms to all orders in the parton-shower approximation and to include non-perturbative effects such as hadronization and the underlying event. The ATLAS generator tunes from 2009 (MC09′[2] [21]) and from 2010 (AUET1 [22]) are used. Additional tunes have been investigated to assess the impact of the underlying-event and parton-shower tuning. With comparable underlying-event tunes and ALPGEN parameters, the comparison between ALPGEN+PYTHIA and ALPGEN+HERWIG/ JIMMY uncovers differences that may arise from different parton-shower implementations and hadronization models.

SHERPA [23] with its default parameters and renormalization scale scheme from version 1.2.3 is also used to generate events with up to six partons in the final state. This provides an independent matrix-element calculation with a different matching scheme between the matrix element and the parton shower. Detailed studies of individual tunes using SHERPA, however, are not performed in this paper.

[2]The ATLAS MC09′ tune only differs from MC09 tune in the value of one parameter regulating multiple interactions, PARP(82), which is the same used in the MC08 tune [21].

The PYTHIA event generator is also compared to the data to study the limitations of leading-order $2 \to 2$ matrix-element calculations. This generator implements a leading-order matrix-element calculation for $2 \to 2$ processes, p_{T}-ordered parton showers, an underlying-event model for multiple-parton interactions and the Lund string model for hadronization. The MRST2007 modified leading order [24, 25] PDFs interfaced with the AMBT1 [21] generator tune are used in the sample generation.

For the purpose of understanding detector effects, the particles generated in the leading-order Monte Carlo generators are passed through a full simulation of the ATLAS detector and trigger [26] based on GEANT4 [27]. Additional proton–proton collisions are added to the hard scatter in the simulation process to reproduce realistic LHC running conditions. Events and jets are selected using the same criteria in data and Monte Carlo simulations.

For the next-to-leading-order pQCD study, the calculation implemented in NLOJet++ 4.1.2 [28] is used. The renormalization and factorization scales are varied independently by a factor of two in order to estimate the impact of higher order terms not included in the calculation. An additional requirement that the ratio of the renormalization and factorization scales did not differ by more than a factor of two was imposed. Two next-to-leading-order PDF sets, CTEQ 6.6 [29] and MSTW 2008 NLO [25], are used for calculating the central values. Only results obtained with the MSTW 2008 NLO PDF set are shown in the paper since the results obtained with the CTEQ 6.6 PDF set are compatible. The 90% confidence-limit error sets are used in the evaluation of the PDF uncertainties. The uncertainty in the calculations due to the uncertainty in the value of α_S is determined by varying the value of α_S by ± 0.002 for each PDF set.

The NLOJet++ program implements a matrix-element calculation, and therefore it lacks a parton-shower interface and does not account for non-perturbative effects. To compare to particle-level measurements, a correction factor is required. PYTHIA and HERWIG++ [30] are used to generate samples without underlying event. Jets in these samples are reconstructed from partons after the parton shower, and observables are compared to those obtained at the particle level in the standard HERWIG++ and PYTHIA samples. A multiplicative correction is calculated

$$C_{\text{non-pert}} = \frac{o_{\text{UE}}^{\text{particle}}}{o_{\text{no UE}}^{\text{parton}}}, \tag{1}$$

where o is the observable of interest calculated at the particle or parton level in the samples with and without underlying event. The correction factor takes the next-to-leading-order pQCD calculations to the particle level. This correction is calculated in three different samples. The correction obtained using the PYTHIA AMBT1 sample is taken as the

Table 1 Different Monte Carlo generators and tunes used for the leading-order analysis in this paper. The asterisk indicates the samples used to determine the uncertainties on the non-perturbative correction to the next-to-leading-order pQCD calculations

Generator	PDF	Tune
ALPGEN+HERWIG/JIMMY	CTEQ6L1 [14]	AUET1 [22]
ALPGEN+PYTHIA	CTEQ6L1 [14]	MC09′ [21]
PYTHIA	MRST2007 LOmod [24, 25]	AMBT1 [21]
PYTHIA*	MRST2007 LOmod [24, 25]	MC09 [21]
SHERPA	CTEQ66 [29]	Default (v1.2.3)
HERWIG++*	MRSTMC al [24, 25]	Default (v2.5)

default value for the analysis, and the systematic uncertainty is estimated from the maximum spread compared to the results from the other models (marked with an asterisk in Table 1). The size of this correction is less than 5% in all observables studied in the next-to-leading-order pQCD analysis. The total uncertainty quoted on the next-to-leading-order pQCD calculations comes from the quadrature sum of the uncertainties from the renormalization and factorization scales, the proton PDFs, α_S and the non-perturbative corrections.

Table 1 presents a summary of the different Monte Carlo generators and tunes that the data are compared to in this paper.

5 Event selection and reconstruction

5.1 Trigger selection

A set of ATLAS first level (level-1) multi-jet triggers is used to select events for the analysis. Multi-jet triggers require several jets reconstructed with a level-1 sliding window algorithm. All multi-jet triggers are symmetric, meaning that each trigger had one particular transverse energy threshold and that this threshold was the same for all jets in an event. Only two-jet and three-jet triggers were needed for the analysis.

The single-jet triggers with a 10 GeV level-1 threshold have been shown to be fully efficient for events with at least one anti-k_t jet with $R = 0.4$ and calibrated $p_T > 60$ GeV [31] using events triggered with the minimum bias triggers. The efficiency for triggering on the leading jet is calculated using the minimum bias triggers. Then, the efficiency of the trigger to fire on the second leading jet is calculated by requiring that the leading jet passes the single-jet trigger. Similarly, the efficiency of the third leading jet is studied by requiring that the second leading jet is matched to a jet trigger object, and the event passes a two-jet trigger. For $p_T > 60$ GeV, events are selected on the trigger plateau.

Figure 1 shows the efficiency for the third leading jet to fire the three-jet trigger as a function of the reconstructed jet p_T for jets of $R = 0.4$ (a) and $R = 0.6$ (b). The efficiencies calculated in data are compared to those from the Monte Carlo detector simulation. The efficiency as a function of jet rapidity is also shown for $R = 0.4$ jets (c) for $p_T > 60$ GeV. A small inefficiency is present in the data at $y = \pm 1.5$. In this transition region between the barrel and end-cap calorimeters the level-1 trigger energy sums did not span between the calorimeters for the early data used here, resulting in this small efficiency drop, which is not modeled by the Monte Carlo simulation. The simulation is not corrected for this effect, since its impact in the measurements is negligible, and included as part of the systematic uncertainties in the data correction described in Sect. 6.

The event-level efficiency as a function of the closest distance between two selected $R = 0.4$ offline jets for events selected using the three-jet trigger is shown in Fig. 1(d). The study probes possible topological dependences in the trigger. A dependence at low ΔR is observed, where $\Delta R = \sqrt{\Delta\phi^2 + \Delta\eta^2}$ represents the minimum separation between selected jets in the event. The dependence on ΔR is well described by the Monte Carlo simulation. For the calculation of the efficiency in the data, the two leading jets are associated with level-1 jet objects and an assumption is made that any topological inefficiency will only affect one of the level-1 jet objects. Figure 1(d) indicates that events in which two jets are separated by $\Delta R < 0.6$ have an efficiency of less than 100%. This inefficiency appears to depend weakly on the jet p_T and is well described in the detector simulation for events where the closest distance between selected jets is greater than 0.45. The inefficiency is accounted for in the Monte Carlo-based data correction described in Sect. 6. Such an inefficiency is not observed in the analysis of jets reconstructed using the anti-k_t algorithm with resolution parameter $R = 0.6$.

The three-jet trigger operated without pre-scaling for the entire data collection period used in this paper. All events falling in the three-jet inclusive multiplicity bin are, therefore, selected using the three-jet trigger with a jet threshold of 10 GeV on the level-1 jet objects. On the other hand, a large pre-scaling was applied to certain two-jet triggers. In order to select events in the two-jet *inclusive* multiplicity bin, several two-jet triggers were used. Three two-jet triggers with symmetric transverse energy thresholds of 10, 15 and 30 GeV were combined independently, weighted by the integrated luminosity associated with each trigger. The three

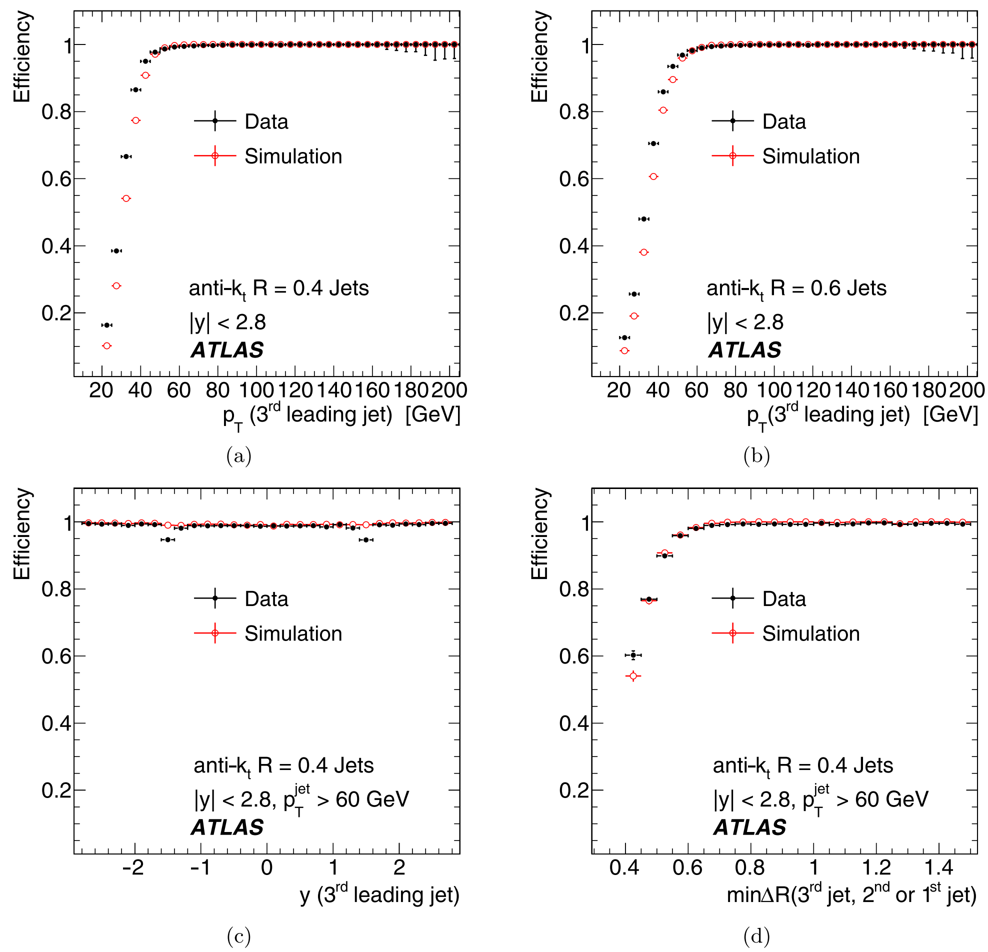

Fig. 1 Jet trigger efficiency for the third leading jet as a function of p_T for anti-k_t jets with $R = 0.4$ (**a**), and $R = 0.6$ (**b**). Jet trigger efficiency as a function of y of the third leading jet with $p_T > 60$ GeV and $R = 0.4$ (**c**). Jet trigger efficiency as a function of the minimum separation ΔR between the two closest jets (**d**). The efficiency is shown both as calculated in data, as described in the text, and in Monte Carlo simulations for the three-jet trigger with a level-1 cut on the jet transverse energy of 10 GeV

triggers were combined in such a way that only one of them was responsible for counting events for which the p_T of the second leading jet was in a particular range. Specifically, the three triggers with thresholds of 10, 15 and 30 GeV covered the ranges of second leading jet p_T of 60–80 GeV, 80–110 GeV and greater than 110 GeV, respectively. The two-jet triggers have an efficiency higher than 99% to select such events.

5.2 Vertex reconstruction

The primary vertex or vertices are found using tracks that originate near the beam collision spot [32], satisfy quality criteria [33] and have transverse momentum above 150 MeV. A vertex is seeded by searching for the global maximum in the distribution of z coordinates of reconstructed tracks. The vertex is fitted using the position of this seed along with neighboring tracks. Tracks incompatible with the reconstructed vertex are used to seed new vertices until no tracks are left. This analysis only uses events in which at least one primary vertex with at least five associated tracks has been reconstructed. No cut on the primary vertex position is applied. The *event* vertex is defined as the vertex in the event for which the sum of the p_T of the tracks associated to that vertex is largest.

5.3 Jet reconstruction

Topological clusters of calorimeter energy evaluated at the electromagnetic scale [31] are used as inputs to the jet finding algorithm. These clusters use the baseline calibration derived from test beams and from $Z \rightarrow ee$ data [34], which reconstructs the energy of particles interacting electromagnetically. The anti-k_t algorithm [9] with resolution parameters $R = 0.4$ and $R = 0.6$ and full four-momentum recombination is used to reconstruct jets from clusters. The jet four-momentum is calculated assuming that the jet origin is at the position of the event vertex. The jet reconstruction is fully efficient in the Monte Carlo simulation for jets with transverse momentum above 30 GeV. The reconstruction efficiency in the simulation compares well with the one measured with data [31].

5.4 Jet energy scale calibration

Jets reconstructed at the electromagnetic scale are measured to have an energy which is lower than the true energy of

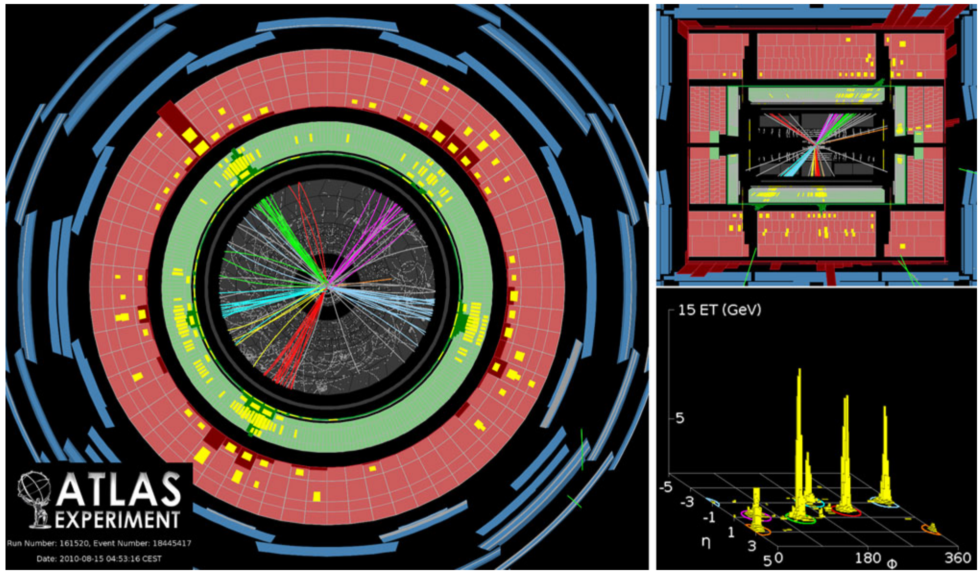

Fig. 2 Event display of a six-jet event satisfying the analysis requirements. The towers in the *bottom right figure* represent transverse energy deposited in the calorimeter projected on a grid of η and ϕ. Jets with transverse momenta ranging from 84 to 203 GeV are measured in this event

interacting particles within the jet. The difference between a hadron-level jet and an electromagnetic-scale jet is due to the different calorimeter response to electromagnetic objects compared to strongly interacting objects, detector induced showering and energy deposition in regions of the detector that are not instrumented. A Monte Carlo-based calibration that corrects for these effects as a function of p_T and y is used to obtain jets with the correct energy scale [35].

5.5 Jet selection criteria

Jets considered in the analysis are selected using the following kinematic and data quality selection criteria:

1. The event must contain at least one jet with $|y| < 2.8$ and a p_T greater than 80 GeV.
2. Jets are required to have $|y| < 2.8$ and $p_T > 60$ GeV in order to be counted.
3. A series of jet cleaning cuts were applied to eliminate various detector effects and suppress beam and other non-collision backgrounds. Overall, these cuts reduce the total number of jets by less than 0.1%. These cuts have been shown to be efficient in eliminating noise, while rejecting a negligible number of true jets.
4. In order the reduce the effects from pileup events, jets are only accepted if at least 70% of their charged particle p_T comes from the event vertex. The charged particle p_T is calculated as the scalar sum of the p_T of reconstructed tracks within a ΔR equal to the resolution parameter used in the jet reconstruction. Overall, this cut lowers the number of selected two-jet events by 0.4%, and its effect increases with jet multiplicity. The cut reduces the number of selected six-jet events by 3.4%. All observables show a negligible dependence on the number of reconstructed primary vertices once this cut is applied [36]. Jets with no charged particle content are accepted, but only constitute a few percent of events at low p_T.
5. Only events with at least two selected jets are used in the analysis.

Table 2 Number of selected events using the criteria described in this paper as a function of inclusive jet multiplicity for jets reconstructed with the anti-k_t algorithm with resolution parameter $R = 0.4$ before correcting for trigger pre-scales

Inclusive multiplicity	Number of events
≥2	500,148
≥3	112,740
≥4	10,999
≥5	1,100
≥6	115

For illustrative purposes, Fig. 2 presents an event display of a six-jet event passing all selection cuts. The transverse energy deposition in the calorimeter is shown as a function of η and ϕ. For this event, the six selected jets are well separated spatially.

Table 2 presents the total number of multi-jet events versus inclusive jet multiplicity. No correction for trigger prescales in the two-jet bin has been applied to the numbers in the table.

6 Data correction for efficiencies and resolution

A correction is needed to compare the measurements to theoretical predictions. The correction, which accounts for trigger inefficiencies, detector resolutions and other detector effects that affect the jet counting, is performed in a single

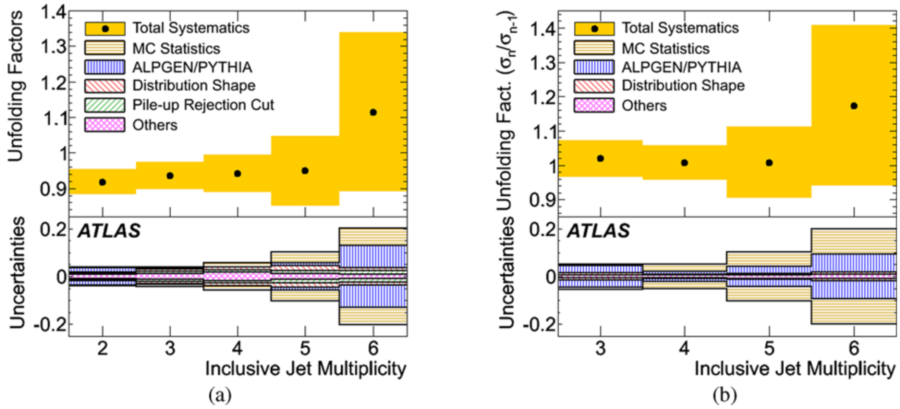

Fig. 3 (Color online) Bin-by-bin correction factors for the cross sections (**a**) and for the n to $n-1$ cross-section ratios (**b**) as a function of the inclusive jet multiplicity. The correction factors calculated using the ALPGEN+HERWIG/JIMMY AUET1 sample are shown with the systematic uncertainty as a *yellow band around the points*. See the text for an explanation of the legend labels

step using a bin-by-bin multiplicative factor calculated from Monte Carlo simulations. For each measured distribution, the corresponding Monte Carlo simulation cross section using truth jets as defined in Sect. 3 is evaluated in the relevant bins, along with the equivalent distributions obtained after the application of detector simulation and analysis cuts. The ratio of the true to the simulated distributions provides the multiplicative correction factor to be applied to the measured distributions. The bins are chosen so that bin migrations due to resolution effects are small. Typically, above 70% of events in a bin built using reconstructed quantities come from the same bin using particle-level quantities in the simulation. A similar fraction of events in a given truth bin fall in the same bin using reconstructed quantities. These fractions, which characterize bin migrations, become smaller with increasing jet multiplicity, but never become less than 0.6.

To perform the correction, the ALPGEN+HERWIG/JIMMY AUET1 Monte Carlo simulation is used. The sample includes, on average, two additional soft proton–proton collision events overlapping with the hard scatter simulated by ALPGEN. The data have fewer overlapping collisions, as revealed by the distribution of the number of selected vertices, and the Monte Carlo simulation is subsequently weighted to match the distribution from the data. The truth distribution is independent of the additional collisions, since jets are built using particles simulated by the ALPGEN+HERWIG/JIMMY Monte Carlo simulation only. Distributions in the Monte Carlo simulation are not further reweighted to match the data. The impact of differences in shapes between data and Monte Carlo simulation on the calculation of the correction factors is instead considered part of the systematic uncertainties in these factors.

The uncertainty in the correction factors is estimated taking into account several effects. One arises from the spread in correction factors coming from different generators (ALPGEN+HERWIG/JIMMY AUET1 and PYTHIA AMBT1). A second detailed study is performed in which the simulated jet p_{T}, y and ϕ resolution is varied according to their measured uncertainties [37, 38]. Third, the shape of the simulated distributions is varied within limits set by the present measurements in order to account for possible biases caused by the input distributions. Samples with a trigger inefficiency in the crack region, with different pile-up rejection cuts and different primary vertex multiplicity distributions are also used to estimate the uncertainty arising from trigger effects and from the impact of overlapping proton–proton collisions. All these effects impact the systematic uncertainties in the correction factors, and their uncertainties are ultimately added in quadrature to provide the final systematic uncertainty in the bin-by-bin correction. Although only important for particular bins, statistical uncertainties on the correction factors are added to the total uncertainty. Results for the bin-by-bin correction factors are presented in Fig. 3. The corresponding uncertainties are calculated for the cross section (a) and for the n to $n-1$ cross-section ratios (b) as a function of the inclusive jet multiplicity. The combined systematic uncertainty is shown as a yellow band around the correction factors. The main components contributing to the systematic uncertainty are shown at the bottom of each figure. The uncertainty in the correction factors for detector efficiencies and resolutions is smaller for most bins and observables than the uncertainty coming from the jet energy scale calibration, discussed in the next section.

The systematic uncertainties in the luminosity calculation affect all cross section measurements, but cancel out in all measurements where cross-section ratios are involved. The integrated luminosity of the dataset used in this paper is measured to be $2.43 \pm 0.08\ \mathrm{pb}^{-1}$ [39] and the associated uncertainty is not shown in the figures.

7 Uncertainty on the jet energy scale

The jet energy scale uncertainty is the dominant uncertainty for most results presented in this paper. The fact that cross sections fall steeply as a function of jet p_{T} implies that even a relatively small uncertainty in the determination of the jet

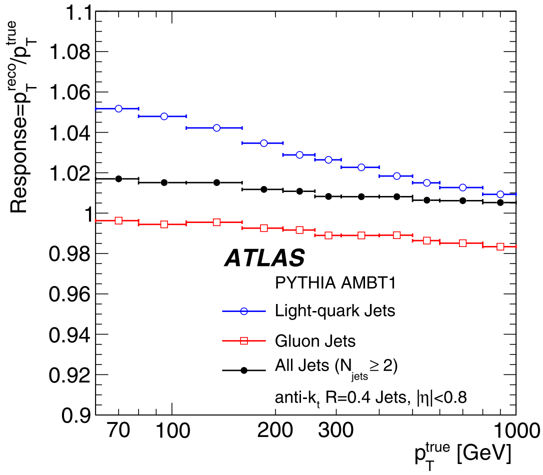

Fig. 4 Jet response (mean reconstructed jet p_T over true jet p_T) as a function of the true p_T for jets tagged as originating from a light quark or a gluon. The jet response in a sample with at least two jets of $p_T > 60$ GeV (and with those two jets within $|y| < 2.8$) is also shown for those jets with $|\eta| < 0.8$. The anti-k_t algorithm with $R = 0.4$ is used

p_T translates into a substantial change in the cross sections as events migrate along the steeply falling curve.

The jet energy scale and its uncertainty [35] have been determined for jets from a dijet sample without nearby activity in the calorimeter. For a multi-jet analysis, additional systematic uncertainties need to be considered. These uncertainties arise from the difference in the calori- meter response to jets of different flavors as well as the impact of the presence of nearby activity in the calorimeter on the jet energy measurement.

Figure 4 shows the calorimeter p_T response for light-quark and gluon jets in the region $|\eta| < 0.8$ as a function of the true jet p_T calculated using the PYTHIA AMBT1 Monte Carlo simulation sample. The response for jets in the two-jet inclusive multiplicity bin is also shown. Light-quark and gluon jets were tagged using the highest-energy parton found in the Monte Carlo simulation particle record within a cone of radius equal to the resolution parameter of the jet algorithm. Only jets that had no additional reconstructed jet of $p_T > 7$ GeV evaluated at the electromagnetic scale within $\Delta R = 1.0$ from the jet axis were used in order to decouple effects in the response caused by jet flavor from effects related to the presence of nearby calorimeter activity.

The Monte Carlo simulation shows a slightly higher fraction of jets matched to gluons for high-multiplicity final states, particularly in the ALPGEN samples. To the extent that the Monte Carlo simulation reflects the data, the difference in response as a function of multiplicity is accounted for in the bin-by-bin correction for efficiencies and resolution.

An additional jet energy scale uncertainty, however, could arise, since the standard jet energy scale was derived for a particular admixture of light-quark and gluon jets. For a different admixture, the jet energy scale uncertainty could be different. In what follows, this uncertainty is referred to as the 'flavor response' uncertainty. This uncertainty is estimated using Monte Carlo simulations [35] by studying the difference between the gluon and light-quark jet response under various assumptions. However, the relative change of the light-quark jet response with respect to the gluon jet response is found to be negligible in all simulations studied [40], so the effect can be safely ignored.

In addition, the fraction of light-quark and gluon jets in multi-jet samples in the data could differ from the fraction predicted by the Monte Carlo simulations, thus leading to a systematic shift in the jet energy scale. The precision with which the flavor composition of the sample is known thus also affects the precision of the jet energy measurement. The flavor composition depends on many theoretical aspects in the event production (parton distribution functions, limitations of leading-order calculations, initial and final state radiation tuning) and the uncertainty in the predictions is not easy to estimate using Monte Carlo simulations. The uncertainty is determined using a data-driven method that provides a measurement of the flavor composition up to the four-jet inclusive multiplicity bin and for jets of $p_T < 210$ GeV [40]. The method uses template fits to the distribution of jet widths and to the number of tracks associated with jets in bins of η, p_T, jet isolation and jet multiplicity. The templates are obtained using Monte Carlo simulations modified to match the distributions found in the two-jet bin. Using these template fits, the measurement of the flavor composition is determined to an accuracy of $\approx 10\%$. Overall, ALPGEN predicts the correct flavor composition to within 30% in bins where the number of collected events is enough to perform the fits. At high p_T and high multiplicities the flavor composition is assumed to be unknown when calculating the jet energy scale uncertainty.

Jets with nearby activity have different properties than the jets used to estimate the jet energy scale uncertainty. In addition, the fraction of jets with nearby activity increases with jet multiplicity. Figure 5 gives the probability of a selected jet occurring within $\Delta R = 1.0$ of a reconstructed jet with $p_T > 7$ GeV at the electromagnetic scale as a function of inclusive jet multiplicity. The overlap probability increases with jet multiplicity, a trend which is reproduced by the simulations.

Jets with nearby activity have a different jet energy scale, as has been demonstrated in Monte Carlo simulations [41]. The systematic uncertainty on their energy scale has been evaluated by studying the correlation between the p_T of the tracks associated to the jet and the p_T measured in the calorimeter, and contributes to the final uncertainty in the jet energy scale used in this analysis.

Approximately 40% of the selected events have more than one vertex in the interaction, indicating the presence

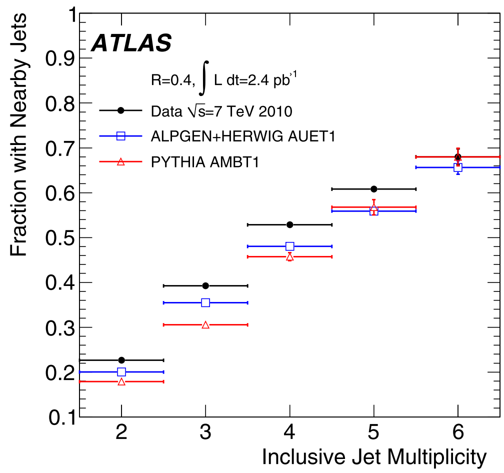

Fig. 5 Fraction of selected jets in each inclusive multiplicity bin with neighboring jets within $\Delta R = 1.0$. Data (*solid circles*) are compared to the ALPGEN+HERWIG/JIMMY AUET1 (*open squares*) and PYTHIA AMBT1 (*open triangles*) Monte Carlo simulations

of additional proton–proton interactions. The vertex multiplicity is low enough that, with a luminous region of several mm and a vertex reconstruction resolution of a few hundred μm, the impact of merged vertices on the analysis is negligible. For the instantaneous luminosities considered in this paper, the probability that two hard events would occur at the same time is negligible. However, a soft interaction occurring in parallel with the hard interaction can produce a contamination of energy from a nearby soft jet. The average effect of these overlapping interactions on the jet energy scale is accounted for by an offset correction, and the systematic uncertainty on that correction has been evaluated [42]. The impact of this uncertainty on the overall jet energy scale uncertainty used in this analysis is negligible for the vast majority of events. The overlapping interactions can also impact the jet counting since the resolution of the jet energy reconstruction depends on the instantaneous luminosity. The effect becomes small after performing a cut on the fraction of charged particle p_T that originates from the event vertex and that is associated to the jet, as described in Sect. 5. The Monte Carlo simulation has been shown to describe tracks within jets [43] and general features of events with pile-up interactions [42]. An uncertainty due to the efficiency of the cut has been estimated in Sect. 6.

In summary, the jet energy scale uncertainty is primarily made of three components: the uncertainty calculated for isolated jets, the uncertainty caused by the presence of nearby calorimeter deposits, and the flavor composition uncertainty. The uncertainty on the energy scale of isolated jets is the largest contributor to the total uncertainty in most bins, except for jets in the five and six-jet bins and of $p_T < 200$ GeV, for which the flavor composition uncertainty is comparable. The positive systematic uncertainty on the jet energy scale of isolated jets falling in the barrel and in high-multiplicity bins varies from 5% at 60 GeV to 2.5% at 1 TeV. In the three-jet and four-jet bins, where the flavor composition is better constrained, the systematic uncertainty is at most 3.5%. The negative systematic uncertainty is smaller and $\approx 3\%$ across all p_T in the barrel. The impact of nearby calorimeter deposits is small, increasing the overall uncertainty by at most 1%. The uncertainty is propagated to the measured distributions using the ALPGEN+HERWIG/JIMMY Monte Carlo simulation and varying the p_T of all jets in the event up or down according to the estimated uncertainties. The use of the same procedure in the data yields comparable results, but the results obtained in the Monte Carlo simulation are favored to eliminate the impact of statistical uncertainties in the data in bins with few events.

8 Results

In this section, measurements[3] corrected to the particle level are compared to theoretical predictions. For comparisons to leading-order Monte Carlo simulations, the anti-k_t algorithm with resolution parameter $R = 0.4$ is used to define a jet. In Figs. 6–10 and 12(b), the darker (orange) shaded error band bracketing the measured cross section corresponds to the total systematic uncertainty, evaluated by adding the individual systematic uncertainties in quadrature but excluding the uncertainty coming from the luminosity measurement. The ratio of the predictions from the Monte Carlo simulations to the measurements is shown at the bottom of each figure. For Figs. 6, 8 and 9, the lighter (grey) error band that appears in the ratio of the predictions from the Monte Carlo simulations to the measurements represents the total systematic uncertainty on the shape of the measured distributions.

Only a few representative Monte Carlo simulations that were studied are shown in the figures and tables. All Monte Carlo simulations are normalized to the measured inclusive two jet cross section. The normalization factors applied to the Monte Carlo simulations studied are given in Table 3, and distinctive features of some of the Monte Carlo simulations not shown are discussed when relevant. Most ALPGEN Monte Carlo simulations predict an inclusive multi-jet cross section similar to the measured cross section, while the PYTHIA Monte Carlo simulation requires scaling factors which differ the most from unity. The differences in the normalization factors between ALPGEN+PYTHIA MC09′ and ALPGEN+HERWIG/JIMMY AUET1 illustrate differences between PYTHIA and HERWIG/JIMMY and their interplay

[3] All measurements in this section have been compiled in tables that can be found in HEPDATA. The NLO pQCD calculation results are also presented in the tables when applicable.

Table 3 Normalization factors applied to each of the Monte Carlo simulations in order to match the measured inclusive two-jet cross section

Leading-order Monte Carlo	Normalization factor
ALPGEN+HERWIG AUET1	1.11
ALPGEN+PYTHIA MC09′	1.22
PYTHIA AMBT1	0.65
SHERPA	1.06

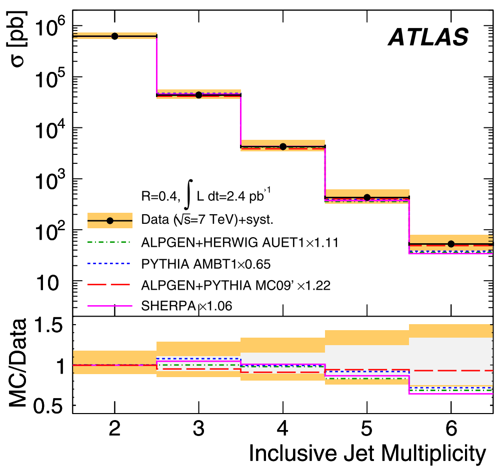

Fig. 6 Total inclusive jet cross section as a function of multiplicity. The data are compared to leading-order Monte Carlo simulations (ALPGEN+HERWIG AUET1, ALPGEN+PYTHIA MC09′, PYTHIA AMBT1 and SHERPA) normalized to the measured inclusive two-jet cross section. The *darker* (*orange*) *shaded* error bands correspond to the systematic uncertainties on the measurement, excluding the luminosity uncertainty. The *lighter* (*grey*) *shaded* error band corresponds to the systematic uncertainty on the shape of the measured distribution. A plot of the ratio of the different Monte Carlo simulations to the data is presented at the *bottom of the figure*

with the matrix-element and parton-shower matching implemented in ALPGEN. The normalization factor for SHERPA is found to be the closest to unity.

Figure 6 shows the results for the cross section as a function of the inclusive jet multiplicity. The measurement systematics are dominated by the jet energy scale uncertainty and range from 10–20% at low multiplicities to almost 30–40% at high multiplicities. The Monte Carlo simulation predictions agree with the measured results across the full inclusive multiplicity spectrum, even when comparing just to the shape of the distributions.

A study that reduces significantly the impact of systematic uncertainties is the ratio of the n-jet to $(n-1)$-jet cross section as a function of multiplicity. In this ratio, the impact of the jet energy scale uncertainty is significantly reduced and the uncertainty due to the luminosity cancels out. Figure 7 presents the results for such a study. Both the uncertainties in the data correction for efficiencies and resolutions and the jet energy scale contribute comparably to the total systematic uncertainty, whereas the statistical uncertainties are smaller than the systematic uncertainties, and negligible in most bins. All Monte Carlo simulations are consistent with the measurements at the present precision, yet there is a noticeable spread in the predictions. Differences at the level of 15% are observed between PYTHIA AMBT1 and ALPGEN+PYTHIA MC09′ in the first bin. These differences most likely arise from the difference between the pure parton-shower (with $2 \to 2$ matrix elements) implemented in PYTHIA and the parton-shower-matched matrix-element calculation (with up to $2 \to 6$ matrix elements) implemented in ALPGEN. All ALPGEN+PYTHIA tunes studied are comparable in this measurement.

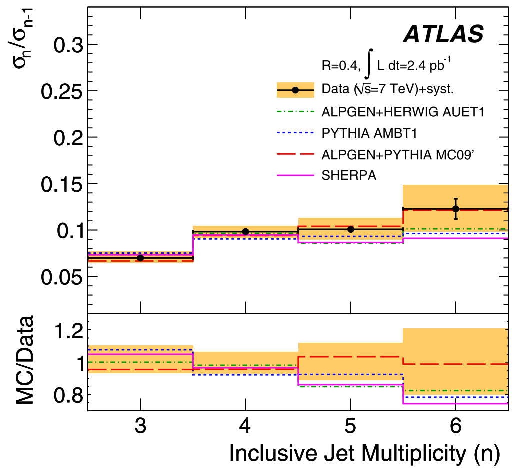

Fig. 7 Ratio of the n-jet cross section to the $(n-1)$-jet cross section for values of n varying from three to six. Systematic uncertainties on the cross section ratios are shown as an error band. Other details are as in the caption to Fig. 6

The differential cross section for multi-jet events as a function of the jet p_T is useful for characterizing kinematic features. The comparison reveals significant differences between the leading order calculations and the measurements. Figure 8 presents the p_T-dependent differential cross sections for the leading, second leading, third leading and fourth leading jet in multi-jet events. The systematic uncertainty in the measurement is 10–20% across p_T and increasing up to 30% for the fourth leading jet differential cross section. The jet energy scale systematic uncertainty remains the dominant uncertainty in the measurement. However, the uncertainty is less than 10% (grey shaded error band) for the leading and second leading jet p_T distributions.

All Monte Carlo simulations agree reasonably well with the data (orange darker shaded error band). However, the PYTHIA AMBT1 Monte Carlo simulation predicts a somewhat steeper slope compared to the data as a function of the leading jet p_T and the second leading jet p_T, whereas the SHERPA and ALPGEN Monte Carlo simulations predict a less steeply falling slope compared to the data. When using

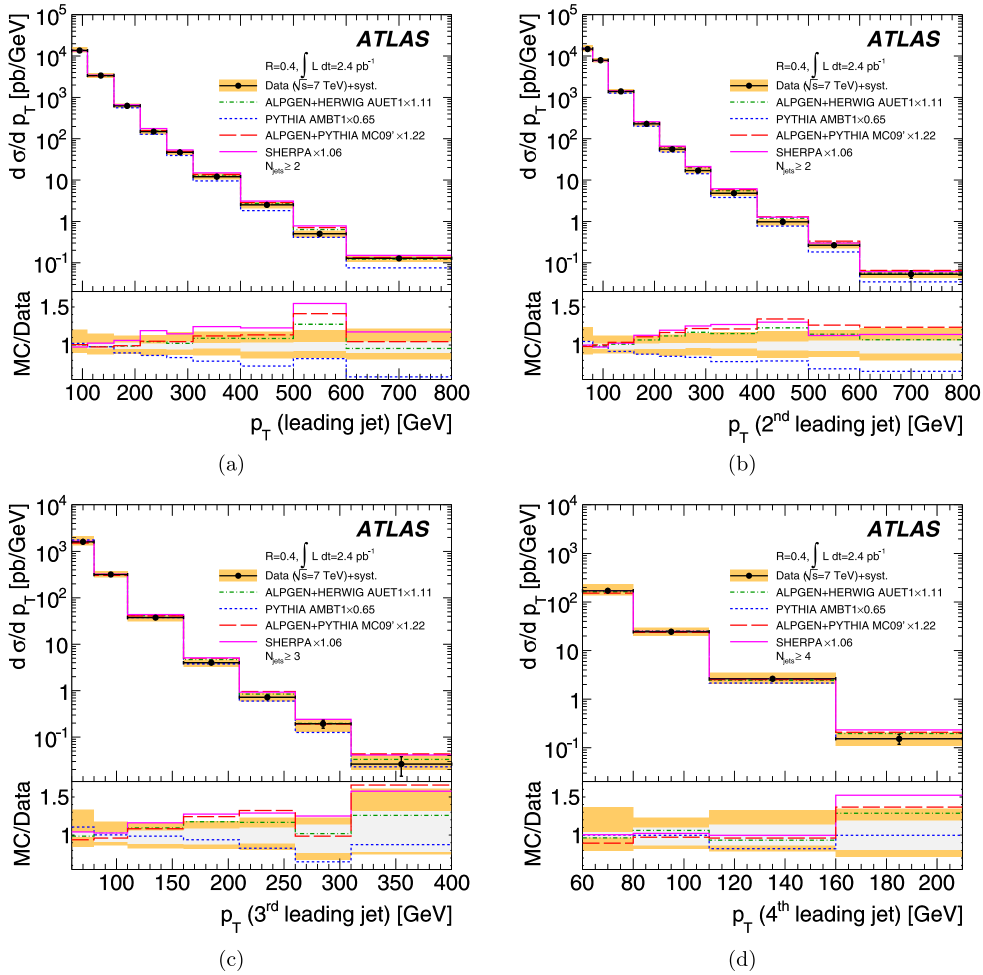

Fig. 8 Differential cross section as a function of leading jet p_T for events with $N_{jets} \geq 2$ (**a**), 2nd leading jet p_T for events with $N_{jets} \geq 2$ (**b**), 3rd leading jet p_T for events with $N_{jets} \geq 3$ (**c**) and 4th leading jet p_T for events with $N_{jets} \geq 4$ (**d**). The results are compared to different leading-order Monte Carlo simulations normalized to the measured inclusive two-jet cross section. Other details are as in the caption to Fig. 6

additional tunes and different PDFs, Monte Carlo simulations using $2 \rightarrow 2$ matrix element calculations, in general, make predictions that fall steeper than what is found in the data, whereas those using $2 \rightarrow n$ matrix element calculations predict less steeply falling spectra.

The differential cross section for multi-jet production as a function of H_T (the scalar sum of the p_T of selected jets in the event) shows similar properties to the differential cross section as a function of p_T. The H_T distributions are typically used for top-quark studies. Figure 9 gives the results for the H_T-dependent differential cross sections for three different multiplicities compared to the ALPGEN, PYTHIA and SHERPA Monte Carlo simulations. Similar conclusions as those reached in the previous figure can be drawn.

A measurement with particular sensitivity to limitations in the leading-order Monte Carlo simulations and NLO pQCD calculations is the ratio of the inclusive three-to-two-jet differential cross section as a function of some characteristic scale in the event. In this measurement, the uncertainty in the luminosity determination cancels out, uncertainties in the jet energy scale are reduced, and statistical uncertainties are limited only by the inclusive three-jet sample.

The three-to-two-jet ratio as a function of the leading jet p_T can be used to tune Monte Carlo simulations for effects due to final state radiation. Figure 10 presents the results on the measurement of the three-to-two-jet cross section ratio as a function of leading jet p_T for jets built with the anti-k_t algorithm using the resolution parameter $R = 0.6$ and with different minimum p_T cuts for all non-leading jets[4]. The cut on the p_T of the leading jet in the event selection is also increased with the minimum p_T cut ($p_T^{lead} > 110$ GeV is used in Fig. 10(b) and $p_T^{lead} > 160$ GeV in Fig. 10(c)). The systematic uncertainties on the measurement are small ($\sim$5%), except in the lowest p_T bin, where uncertainties in the data correction for efficiencies and resolutions and the jet energy scale dominate. ALPGEN+HERWIG AUET1 and ALPGEN+PYTHIA MC09′ describe the data well, and the agreements are largely independent of the tunes chosen. SHERPA also describes the data well. PYTHIA AMBT1 predicts a higher ratio than that measured over the p_T range from 200 GeV to 600 GeV. The disagreement is similar

[4]Results (not shown) were also obtained using $R = 0.4$ and are compiled in tables in HEPDATA.

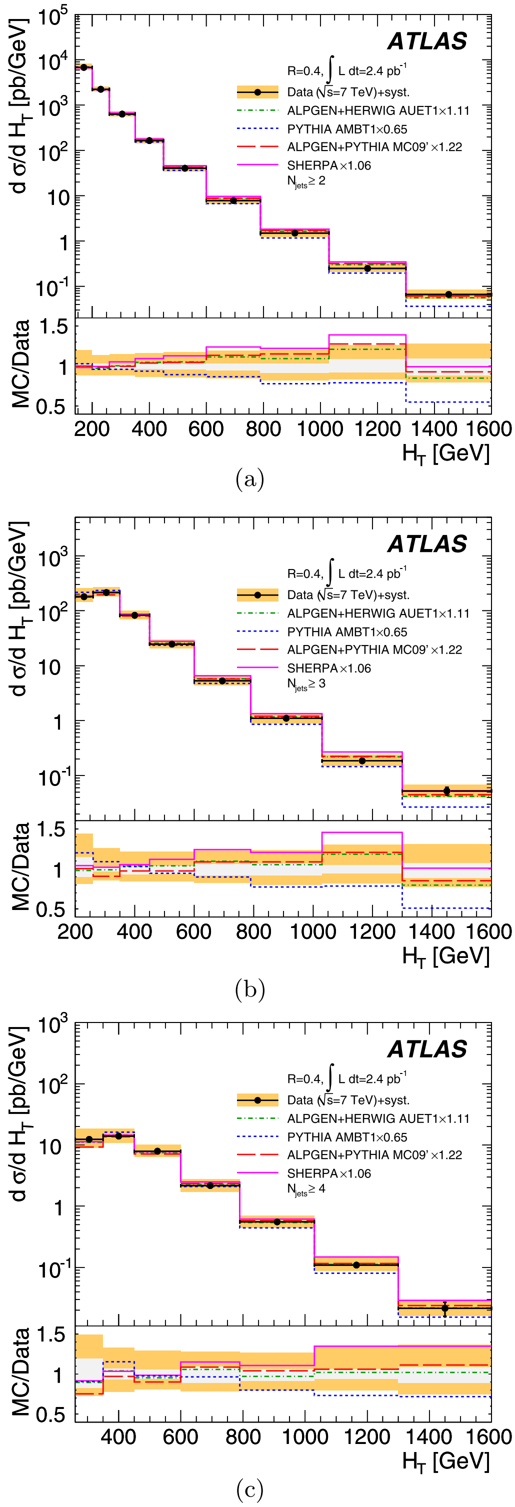

Fig. 9 Differential cross section as a function of H_T for events with at least two selected jets (**a**), three selected jets (**b**) and four selected jets (**c**). The results are compared to different leading-order Monte Carlo simulations normalized to the measured inclusive two-jet cross section. Other details are as in the caption to Fig. 6

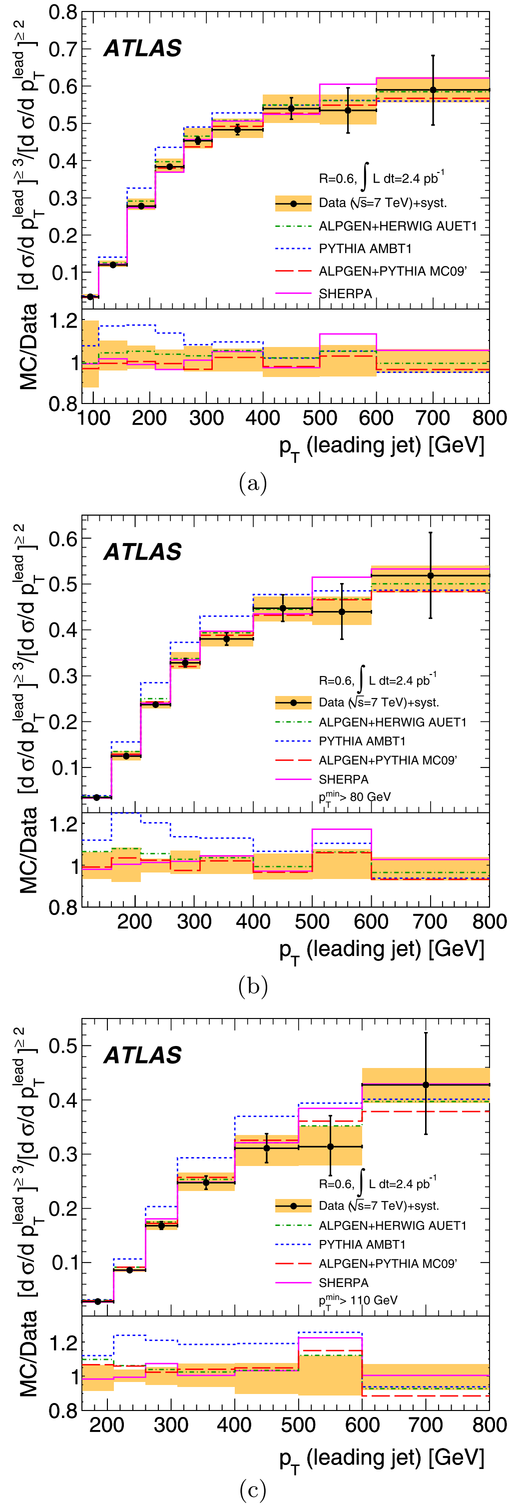

Fig. 10 Three-to-two-jet differential cross-section ratio as a function of the leading jet p_T. In the figures, a resolution parameter $R = 0.6$ is used. The three figures contain a minimum p_T cut for all non-leading jets of (**a**) 60 GeV, (**b**) 80 GeV and (**c**) 110 GeV. The results are compared to leading-order Monte Carlo simulations. Other details are as in the caption to Fig. 6

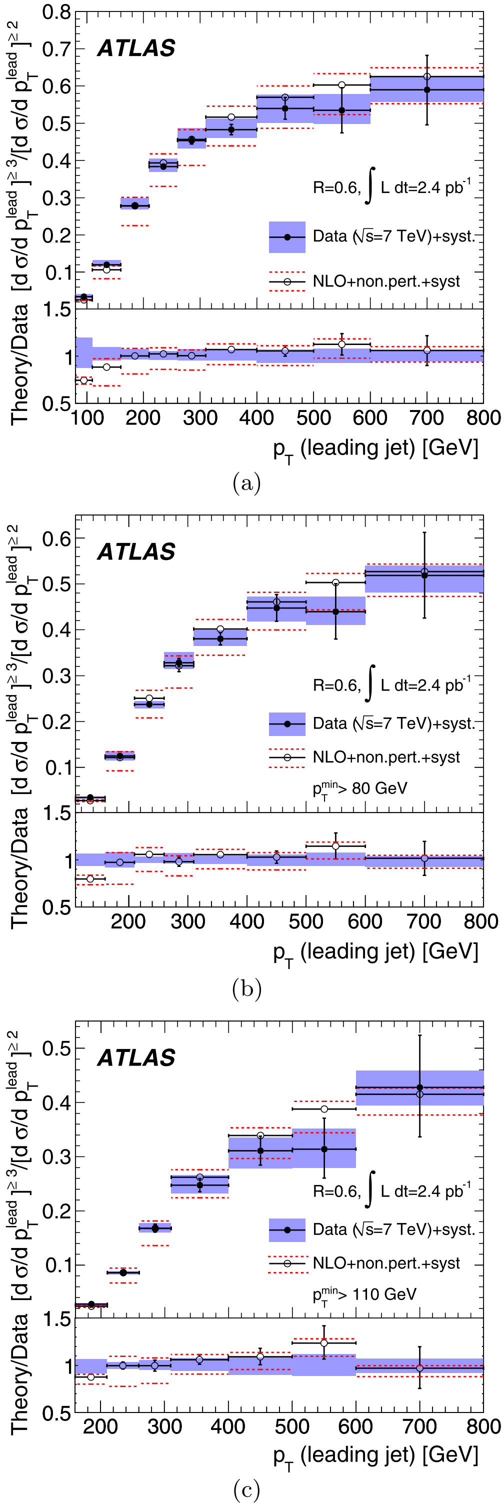

Fig. 11 (Color online) Three-to-two-jet differential cross-section ratio as a function of the leading jet p_T. In the figures a resolution parameter $R = 0.6$ is used. The three figures contain a minimum p_T cut for all non-leading jets of (**a**) 60 GeV, (**b**) 80 GeV and (**c**) 110 GeV. The results are compared to a NLO pQCD calculation with the MSTW 2008 NLO PDF set. The data error bands are identical to the results shown in Fig. 10. The systematic uncertainties on the theoretical prediction are shown as *dotted red lines* above and below the theoretical prediction

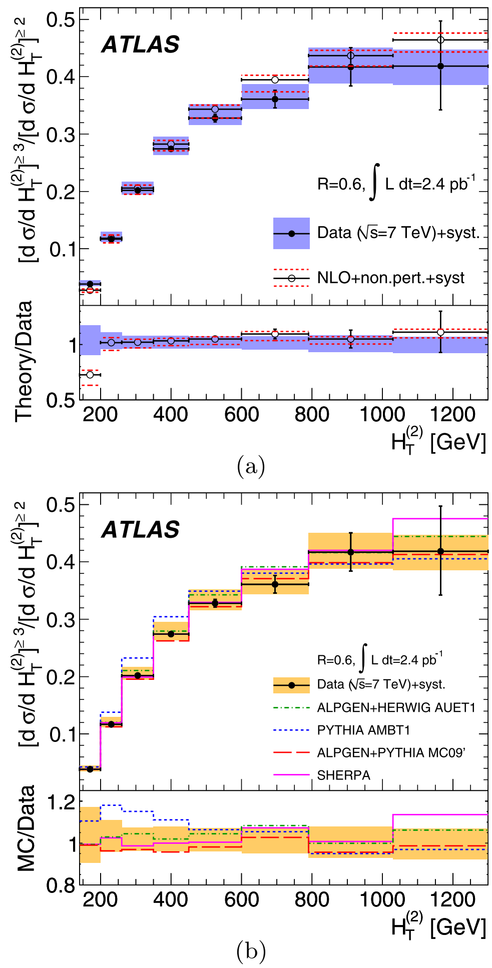

Fig. 12 (Color online) Three-to-two-jet differential cross-section ratio as a function of the sum of the p_T of the two leading jets ($H_T^{(2)}$) using $R = 0.6$. The two figures present the same measurements and error bands. The data are compared to (**a**) a NLO pQCD calculation and (**b**) several leading-order Monte Carlo simulations. The systematic uncertainties on the theoretical prediction for the NLO pQCD calculations are shown as *dotted red lines* above and below the theoretical prediction

when other $2 \to 2$ Monte Carlo simulations with different tunes and PDFs are used. The systematic uncertainty in the lowest p_T bin decreases significantly as the minimum p_T cut is raised to 80 GeV for all jets.

Figure 11 presents the same measurement results as Fig. 10, except the data are now compared to the NLO pQCD calculations corrected for non-perturbative effects. The MSTW 2008 NLO PDF set has been used, but comparable results are obtained with the CTEQ 6.6 PDF set. The systematic uncertainties on the theoretical predictions are shown as dotted red lines above and below the theoretical prediction. The NLO pQCD calculations describe the data well, except in the lowest p_T bin, where there is a large discrepancy. The discrepancy diminishes significantly once the minimum p_T for all jets is raised to 110 GeV and the p_T of the leading jet is required to be greater than 160 GeV.

Additional NLO pQCD calculations of the three-to-two-jet cross section ratio were performed as a function of different kinematic variables, such as H_{T}, the sum of the p_{T} of the two leading jets ($H_T^{(2)}$) and the sum of the p_{T} of the three leading jets. The NLO pQCD calculation for the ratio as a function of $H_T^{(2)}$ was found to give the smallest theoretical scale uncertainty and is, therefore, most sensitive to input parameters such as α_S. Figure 12 shows a comparison of the measurement to both (a) NLO pQCD and (b) leading order calculations for $R = 0.6$. Scale uncertainties of the NLO pQCD calculations are larger for jets with $R = 0.4$ than with $R = 0.6$. The theoretical uncertainty of the NLO pQCD calculations shown in Fig. 12 is comparable to the measurement uncertainties, but is significantly reduced compared to the theoretical uncertainties presented in Fig. 11. With the reduced theoretical uncertainty, the disagreement between data and the NLO pQCD calculations in the lowest $H_T^{(2)}$ bin is now enhanced. Due to the kinematic cuts applied in the analysis, the NLO pQCD calculations only account for the lowest-order contribution to the two-jet cross section in the region where the sum of the first and second leading jet p_{T} is less than 160 GeV. Consequentially, this effective leading-order estimation is subject to large theoretical uncertainties, which might be responsible for the observed discrepancy.

A comparison of the same measurement to leading-order Monte Carlo simulations is given in Fig. 12(b). The general agreement between leading-order Monte Carlo simulations with the measurements follows the same general trends as the comparison of the three-to-two-jet ratio versus leading jet p_{T} shown in Fig. 10.

9 Summary and conclusion

A first dedicated study of multi-jet events has been performed in proton–proton collisions at a center-of-mass energy of 7 TeV using the ATLAS detector with an integrated luminosity of 2.4 pb^{-1}. Leading-order Monte Carlo simulations have been compared to multi-jet inclusive and differential cross sections. The present study extends up to a multiplicity of six jets, up to jet p_{T} of 800 GeV and up to event H_{T} of 1.6 TeV.

For events containing two or more jets with $p_{\mathrm{T}} > 60$ GeV, of which at least one has $p_{\mathrm{T}} > 80$ GeV, a reasonable agreement is found between data and leading-order Monte Carlo simulations with parton-shower tunes that describe adequately the ATLAS $\sqrt{s} = 7$ TeV underlying-event data. The agreement is found after the predictions of the Monte Carlo simulations are normalized to the measured inclusive two-jet cross section.

All models reproduce the main features of the multijet data. The $2 \to 2$ calculations show some departure from the data for the three-to-two jet cross-section ratios, predicting a higher ratio than observed. The $2 \to n$ calculations describe the measured ratios, independent of the tune or parton shower implementation. The shape of the differential cross sections as a function of p_{T} and H_{T}, studied in the inclusive two-jet and three-jet bins, falls off less (more) steeply in the $2 \to n$ ($2 \to 2$) calculations.

A measurement of the three-to-two-jet cross section ratio as a function of the leading jet p_{T} and the sum of the two leading jet p_{T}s is described well by ALPGEN, SHERPA and a NLO pQCD calculation, albeit with a significant discrepancy in the lowest p_{T} bin for the latter comparison. Future comparisons with NLO pQCD calculations will be useful for constraining parameters, such as parton distribution functions or the value of the strong coupling constant, α_S. Systematic uncertainties from the measurement are presently comparable to the theoretical uncertainties, but should be reduced with larger data samples and higher energy collisions.

Acknowledgements We thank CERN for the very successful operation of the LHC, as well as the support staff from our institutions without whom ATLAS could not be operated efficiently.

We acknowledge the support of ANPCyT, Argentina; YerPhI, Armenia; ARC, Australia; BMWF, Austria; ANAS, Azerbaijan; SSTC, Belarus; CNPq and FAPESP, Brazil; NSERC, NRC and CFI, Canada; CERN; CONICYT, Chile; CAS, MOST and NSFC, China; COLCIENCIAS, Colombia; MSMT CR, MPO CR and VSC CR, Czech Republic; DNRF, DNSRC and Lundbeck Foundation, Denmark; ARTEMIS, European Union; IN2P3-CNRS, CEA-DSM/IRFU, France; GNAS, Georgia; BMBF, DFG, HGF, MPG and AvH Foundation, Germany; GSRT, Greece; ISF, MINERVA, GIF, DIP and Benoziyo Center, Israel; INFN, Italy; MEXT and JSPS, Japan; CNRST, Morocco; FOM and NWO, Netherlands; RCN, Norway; MNiSW, Poland; GRICES and FCT, Portugal; MERYS (MECTS), Romania; MES of Russia and ROSATOM, Russian Federation; JINR; MSTD, Serbia; MSSR, Slovakia; ARRS and MVZT, Slovenia; DST/NRF, South Africa; MICINN, Spain; SRC and Wallenberg Foundation, Sweden; SER, SNSF and Cantons of Bern and Geneva, Switzerland; NSC, Taiwan; TAEK, Turkey; STFC, the Royal Society and Leverhulme Trust, United Kingdom; DOE and NSF, United States of America.

The crucial computing support from all WLCG partners is acknowledged gratefully, in particular from CERN and the ATLAS Tier-1 facilities at TRIUMF (Canada), NDGF (Denmark, Norway, Sweden), CC-IN2P3 (France), KIT/GridKA (Germany), INFN-CNAF (Italy), NL-T1 (Netherlands), PIC (Spain), ASGC (Taiwan), RAL (UK) and BNL (USA) and in the Tier-2 facilities worldwide.

References

1. CDF Collaboration, F. Abe et al., Properties of high mass multi-jet events at the Fermilab $p\bar{p}$ collider. Phys. Rev. Lett. **75**, 608 (1995)
2. CDF Collaboration, F. Abe et al., Further properties of high mass multi-jet events at the Fermilab proton–anti-proton collider. Phys. Rev. D **54**, 4221 (1996). arXiv:hep-ex/9605004 [hep-ex]

3. D0 Collaboration, B. Abbott et al., Ratios of multijet cross sections in $p\bar{p}$ collisions at $\sqrt{s} = 1.8$ TeV. Phys. Rev. Lett. **86**, 1955 (2001). arXiv:hep-ex/0009012 [hep-ex]
4. D0 Collaboration, V.M. Abazov et al., Multiple jet production at low transverse energies in $p\bar{p}$ collisions at $\sqrt{s} = 1.8$ TeV. Phys. Rev. D **67**, 052001 (2003). arXiv:hep-ex/0207046 [hep-ex]
5. CMS Collaboration, Measurement of the ratio of the 3-jet to 2-jet cross sections in pp collisions at $\sqrt{s} = 7$ TeV. arXiv:1106.0647
6. The ATLAS Collaboration, The ATLAS experiment at the CERN large hadron collider. J. Instrum. **3**, S08003 (2008).
7. G. Aad et al., ATLAS pixel detector electronics and sensors. J. Instrum. **3**, P07007 (2008)
8. R. Achenbach et al., The ATLAS level-1 calorimeter trigger. J. Instrum. **3**, P03001 (2008)
9. M. Cacciari, G.P. Salam, G. Soyez, The anti-kt jet clustering algorithm. J. High Energy Phys. **04**, 063 (2008)
10. M. Cacciari, G.P. Salam, G. Soyez, http://fastjet.fr/
11. S. Frixione, G. Ridolfi, Jet photoproduction at HERA. Nucl. Phys. B **507**, 315 (1997)
12. The ATLAS Collaboration, Measurement of underlying event characteristics using charged particles in pp collisions at $\sqrt{s} =$ 900 GeV and 7 TeV with the ATLAS detector. Phys. Rev. D **83**, 112001 (2011)
13. M.L. Mangano et al., ALPGEN, a generator for hard multiparton processes in hadronic collisions. J. High Energy Phys. **07**, 001 (2003)
14. J. Pumplin et al., New generation of parton distributions with uncertainties from global QCD analysis. J. High Energy Phys. **07**, 012 (2002)
15. T. Sjostrand, S. Mrenna, P.Z. Skands, A brief introduction to PYTHIA 8.1. Comput. Phys. Commun. **178**, 852 (2008)
16. T. Sjostrand et al., High-energy physics event generation with PYTHIA 6.1. Comput. Phys. Commun. **135**, 238 (2001)
17. G. Corcella et al., HERWIG 6.5: an event generator for hadron emission reactions with interfering gluons (including supersymmetric processes). J. High Energy Phys. **01**, 010 (2001)
18. G. Corcella et al., HERWIG 6.5 release note. arXiv:hep-ph/0210213
19. J.M. Butterworth, J.R. Forshaw, Photoproduction of multi-jet events at HERA: a Monte Carlo simulation. J. Phys. G **19**, 1657 (1993)
20. J.M. Butterworth, J.R. Forshaw, M.H. Seymour, Multiparton interactions in photoproduction at HERA. Z. Phys. C **72**, 637 (1996)
21. The ATLAS Collaboration, ATLAS Monte Carlo tunes for MC09. ATLAS note ATLAS-PHYS-PUB-2010-002 (2010)
22. The ATLAS Collaboration, First tuning of HERWIG/JIMMY to ATLAS data. ATLAS note ATLAS-PHYS-PUB-2010-014 (2010)
23. T. Gleisberg et al., Event generation with SHERPA 1.1. J. High Energy Phys. **02**, 007 (2009)
24. A. Sherstnev, R.S. Thorne, Different PDF approximations useful for LO Monte Carlo generators, arXiv:0807.2132 [hep-ph]
25. A.D. Martin et al., Parton distributions for the LHC. Eur. Phys. J. C **63**, 189 (2009)
26. The ATLAS Collaboration, The ATLAS simulation infrastructure. Eur. Phys. J. C **70**, 823 (2010). arXiv:1005.4568
27. S. Agostinelli et al., Geant simulation. Nucl. Instrum. Methods A **506**, 250 (2003)
28. Z. Nagy, Next-to-leading order calculation of three jet observables in hadron hadron collisions. Phys. Rev. D **68**, 094002 (2003)
29. P.M. Nadolsky et al., Implications of CTEQ global analysis for collider observables. Phys. Rev. D **78**, 013004 (2008). arXiv:0802.0007 [hep-ph]
30. M. Bahr et al., Herwig++ physics and manual. Eur. Phys. J. C **58**, 639 (2008). arXiv:0803.0883 [hep-ph]
31. The ATLAS Collaboration, Measurement of inclusive jet and dijet cross sections in proton–proton collisions at 7 TeV center-of-mass energy with the ATLAS detector. Eur. Phys. J. C **71**, 1512 (2011)
32. The ATLAS Collaboration, Characterization of interaction-point beam parameters using the pp event-vertex distribution reconstructed in the ATLAS detector at the LHC. ATLAS note ATLAS-CONF-2010-027 (2010)
33. The ATLAS Collaboration, Performance of primary vertex reconstruction in proton–proton collisions at $\sqrt{s} = 7$ TeV. ATLAS note ATLAS-CONF-2010-069 (2010)
34. The ATLAS Collaboration, Measurement of the $W \to l\nu$ and $Z/\gamma \to ll$ production cross sections in proton–proton collisions at $\sqrt{s} = 7$ TeV with the ATLAS detector. J. High Energy Phys. **12**, 60 (2010)
35. The ATLAS Collaboration, Final jet energy scale and its systematic uncertainty for jets produced in proton–proton collisions at $\sqrt{s} = 7$ TeV and measured with the ATLAS detector for the 2010 dataset. ATLAS note ATLAS-CONF-2011-032 (2011)
36. The ATLAS Collaboration, Measurements of multi-jet production cross-sections in proton–proton collisions at 7 TeV center-of-mass energy with the ATLAS detector. ATLAS note ATLAS-CONF-2011-043 (2011)
37. The ATLAS Collaboration, Jet energy resolution and reconstruction efficiencies from in-situ techniques with the ATLAS detector using proton–proton collisions at a center of mass energy $\sqrt{s} = 7$ TeV. ATLAS note ATLAS-CONF-2010-054 (2010)
38. The ATLAS Collaboration, Measurement of Dijet azimuthal decorrelations in pp collisions at $sqrt(s) = 7$ TeV. Phys. Rev. Lett. **106**, 172002 (2011)
39. The ATLAS Collaboration, Updated luminosity determination in pp collisions at $\sqrt{s} = 7$ TeV using the ATLAS detector. ATLAS note ATLAS-CONF-2011-011 (2011)
40. The ATLAS Collaboration, Light-quark and gluon jets in ATLAS: calorimeter response, jet energy scale systematics, and sample characterization. ATLAS note ATLAS-CONF-2011-053 (2011)
41. The ATLAS Collaboration, Close-by jet effects on jet energy scale calibration in pp collisions at $\sqrt{s} = 7$ TeV with the ATLAS detector. ATLAS note ATLAS-CONF-2011-062 (2011)
42. The ATLAS Collaboration, In-situ jet energy scale and jet shape corrections for multiple interactions in the first ATLAS data at the LHC. ATLAS note ATLAS-CONF-2011-030 (2011)
43. The ATLAS Collaboration, Properties of jets measured from tracks in proton–proton collisions at center-of-mass energy $\sqrt{s} =$ 7 TeV with the ATLAS detector. arXiv:1107.3311 [hep-ex] (submitted to Phys. Rev. D)

The ATLAS Collaboration

G. Aad[48], B. Abbott[111], J. Abdallah[11], A.A. Abdelalim[49], A. Abdesselam[118], O. Abdinov[10], B. Abi[112], M. Abolins[88], H. Abramowicz[153], H. Abreu[115], E. Acerbi[89a,89b], B.S. Acharya[164a,164b], D.L. Adams[24], T.N. Addy[56], J. Adelman[175], M. Aderholz[99], S. Adomeit[98], P. Adragna[75], T. Adye[129], S. Aefsky[22], J.A. Aguilar-Saavedra[124b,a], M. Aharrouche[81], S.P. Ahlen[21], F. Ahles[48], A. Ahmad[148], M. Ahsan[40], G. Aielli[133a,133b], T. Akdogan[18a], T.P.A. Åkesson[79], G. Akimoto[155], A.V. Akimov[94], A. Akiyama[67], M.S. Alam[1], M.A. Alam[76], S. Albrand[55], M. Aleksa[29], I.N. Aleksandrov[65], F. Alessandria[89a], C. Alexa[25a], G. Alexander[153], G. Alexandre[49], T. Alexopoulos[9], M. Alhroob[20], M. Aliev[15], G. Alimonti[89a], J. Alison[120], M. Aliyev[10], P.P. Allport[73], S.E. Allwood-Spiers[53], J. Almond[82], A. Aloisio[102a,102b], R. Alon[171], A. Alonso[79], M.G. Alviggi[102a,102b], P. Amaral[29], C. Amelung[22], V.V. Ammosov[128], A. Amorim[124a,b], G. Amorós[167], N. Amram[153], C. Anastopoulos[29], N. Andari[115], T. Andeen[34], C.F. Anders[20], K.J. Anderson[30], A. Andreazza[89a,89b], V. Andrei[58a], M.-L. Andrieux[55], X.S. Anduaga[70], A. Angerami[34], F. Anghinolfi[29], N. Anjos[124a], A. Annovi[47], A. Antonaki[8], M. Antonelli[47], S. Antonelli[19a,19b], A. Antonov[96], J. Antos[144b], F. Anulli[132a], S. Aoun[83], L. Aperio Bella[4], R. Apolle[118,c], G. Arabidze[88], I. Aracena[143], Y. Arai[66], A.T.H. Arce[44], J.P. Archambault[28], S. Arfaoui[29,d], J.-F. Arguin[14], E. Arik[18a,*], M. Arik[18a], A.J. Armbruster[87], O. Arnaez[81], C. Arnault[115], A. Artamonov[95], G. Artoni[132a,132b], D. Arutinov[20], S. Asai[155], R. Asfandiyarov[172], S. Ask[27], B. Åsman[146a,146b], L. Asquith[5], K. Assamagan[24], A. Astbury[169], A. Astvatsatourov[52], G. Atoian[175], B. Aubert[4], B. Auerbach[175], E. Auge[115], K. Augsten[127], M. Aurousseau[145a], N. Austin[73], G. Avolio[163], R. Avramidou[9], D. Axen[168], C. Ay[54], G. Azuelos[93,e], Y. Azuma[155], M.A. Baak[29], G. Baccaglioni[89a], C. Bacci[134a,134b], A.M. Bach[14], H. Bachacou[136], K. Bachas[29], G. Bachy[29], M. Backes[49], M. Backhaus[20], E. Badescu[25a], P. Bagnaia[132a,132b], S. Bahinipati[2], Y. Bai[32a], D.C. Bailey[158], T. Bain[158], J.T. Baines[129], O.K. Baker[175], M.D. Baker[24], S. Baker[77], F. Baltasar Dos Santos Pedrosa[29], E. Banas[38], P. Banerjee[93], Sw. Banerjee[169], D. Banfi[29], A. Bangert[137], V. Bansal[169], H.S. Bansil[17], L. Barak[171], S.P. Baranov[94], A. Barashkou[65], A. Barbaro Galtieri[14], T. Barber[27], E.L. Barberio[86], D. Barberis[50a,50b], M. Barbero[20], D.Y. Bardin[65], T. Barillari[99], M. Barisonzi[174], T. Barklow[143], N. Barlow[27], B.M. Barnett[129], R.M. Barnett[14], A. Baroncelli[134a], G. Barone[49], A.J. Barr[118], F. Barreiro[80], J. Barreiro Guimarães da Costa[57], P. Barrillon[115], R. Bartoldus[143], A.E. Barton[71], D. Bartsch[20], V. Bartsch[149], R.L. Bates[53], L. Batkova[144a], J.R. Batley[27], A. Battaglia[16], M. Battistin[29], G. Battistoni[89a], F. Bauer[136], H.S. Bawa[143,f], B. Beare[158], T. Beau[78], P.H. Beauchemin[118], R. Beccherle[50a], P. Bechtle[41], H.P. Beck[16], M. Beckingham[48], K.H. Becks[174], A.J. Beddall[18c], A. Beddall[18c], S. Bedikian[175], V.A. Bednyakov[65], C.P. Bee[83], M. Begel[24], S. Behar Harpaz[152], P.K. Behera[63], M. Beimforde[99], C. Belanger-Champagne[85], P.J. Bell[49], W.H. Bell[49], G. Bella[153], L. Bellagamba[19a], F. Bellina[29], M. Bellomo[119a], A. Belloni[57], O. Beloborodova[107], K. Belotskiy[96], O. Beltramello[29], S. Ben Ami[152], O. Benary[153], D. Benchekroun[135a], C. Benchouk[83], M. Bendel[81], B.H. Benedict[163], N. Benekos[165], Y. Benhammou[153], D.P. Benjamin[44], M. Benoit[115], J.R. Bensinger[22], K. Benslama[130], S. Bentvelsen[105], D. Berge[29], E. Bergeaas Kuutmann[41], N. Berger[4], F. Berghaus[169], E. Berglund[49], J. Beringer[14], K. Bernardet[83], P. Bernat[77], R. Bernhard[48], C. Bernius[24], T. Berry[76], A. Bertin[19a,19b], F. Bertinelli[29], F. Bertolucci[122a,122b], M.I. Besana[89a,89b], N. Besson[136], S. Bethke[99], W. Bhimji[45], R.M. Bianchi[29], M. Bianco[72a,72b], O. Biebel[98], S.P. Bieniek[77], J. Biesiada[14], M. Biglietti[134a,134b], H. Bilokon[47], M. Bindi[19a,19b], S. Binet[115], A. Bingul[18c], C. Bini[132a,132b], C. Biscarat[177], U. Bitenc[48], K.M. Black[21], R.E. Blair[5], J.-B. Blanchard[115], G. Blanchot[29], T. Blazek[144a], C. Blocker[22], J. Blocki[38], A. Blondel[49], W. Blum[81], U. Blumenschein[54], G.J. Bobbink[105], V.B. Bobrovnikov[107], S.S. Bocchetta[79], A. Bocci[44], C.R. Boddy[118], M. Boehler[41], J. Boek[174], N. Boelaert[35], S. Böser[77], J.A. Bogaerts[29], A. Bogdanchikov[107], A. Bogouch[90,*], C. Bohm[146a], V. Boisvert[76], T. Bold[163,g], V. Boldea[25a], N.M. Bolnet[136], M. Bona[75], V.G. Bondarenko[96], M. Boonekamp[136], G. Boorman[76], C.N. Booth[139], S. Bordoni[78], C. Borer[16], A. Borisov[128], G. Borissov[71], I. Borjanovic[12a], S. Borroni[132a,132b], K. Bos[105], D. Boscherini[19a], M. Bosman[11], H. Boterenbrood[105], D. Botterill[129], J. Bouchami[93], J. Boudreau[123], E.V. Bouhova-Thacker[71], C. Boulahouache[123], C. Bourdarios[115], N. Bousson[83], A. Boveia[30], J. Boyd[29], I.R. Boyko[65], N.I. Bozhko[128], I. Bozovic-Jelisavcic[12b], J. Bracinik[17], A. Braem[29], P. Branchini[134a], G.W. Brandenburg[57], A. Brandt[7], G. Brandt[15], O. Brandt[54], U. Bratzler[156], B. Brau[84], J.E. Brau[114], H.M. Braun[174], B. Brelier[158], J. Bremer[29], R. Brenner[166], S. Bressler[152], D. Breton[115], D. Britton[53], F.M. Brochu[27], I. Brock[20], R. Brock[88], T.J. Brodbeck[71], E. Brodet[153], F. Broggi[89a], C. Bromberg[88], G. Brooijmans[34], W.K. Brooks[31b], G. Brown[82], H. Brown[7], P.A. Bruckman de Renstrom[38], D. Bruncko[144b], R. Bruneliere[48], S. Brunet[61], A. Bruni[19a], G. Bruni[19a], M. Bruschi[19a], T. Buanes[13], F. Bucci[49], J. Buchanan[118], N.J. Buchanan[2], P. Buchholz[141], R.M. Buckingham[118], A.G. Buckley[45], S.I. Buda[25a], I.A. Budagov[65], B. Budick[108], V. Büscher[81], L. Bugge[117], D. Buira-Clark[118], O. Bulekov[96], M. Bunse[42], T. Buran[117], H. Burckhart[29], S. Burdin[73], T. Burgess[13], S. Burke[129], E. Busato[33], P. Bussey[53], C.P. Buszello[166], F. Butin[29], B. Butler[143], J.M. Butler[21], C.M. Buttar[53], J.M. Butterworth[77], W. Buttinger[27], T. Byatt[77], S. Cabrera Urbán[167], D. Caforio[19a,19b], O. Cakir[3a], P. Calafiura[14], G. Calderini[78], P. Calfayan[98], R. Calkins[106], L.P. Caloba[23a], R. Caloi[132a,132b], D. Calvet[33], S. Calvet[33], R. Camacho Toro[33], P. Camarri[133a,133b], M. Cambiaghi[119a,119b], D. Cameron[117], S. Campana[29], M. Campanelli[77], V. Canale[102a,102b], F. Canelli[30], A. Canepa[159a], J. Cantero[80], L. Capasso[102a,102b], M.D.M. Capeans Garrido[29], I. Caprini[25a], M. Caprini[25a], D. Capriotti[99], M. Capua[36a,36b], R. Caputo[148], C. Caramarcu[25a], R. Cardarelli[133a], T. Carli[29], G. Carlino[102a], L. Carminati[89a,89b], B. Caron[159a], S. Caron[48], G.D. Carrillo Montoya[172], A.A. Carter[75], J.R. Carter[27], J. Carvalho[124a,h], D. Casadei[108], M.P. Casado[11], M. Cascella[122a,122b], C. Caso[50a,50b,*], A.M. Castaneda Hernandez[172], E. Castaneda-Miranda[172], V. Castillo Gimenez[167], N.F. Castro[124a], G. Cataldi[72a], F. Cataneo[29], A. Catinaccio[29], J.R. Catmore[71], A. Cattai[29], G. Cattani[133a,133b], S. Caughron[88], D. Cauz[164a,164c], P. Cavalleri[78], D. Cavalli[89a],

M. Cavalli-Sforza[11], V. Cavasinni[122a,122b], F. Ceradini[134a,134b], A.S. Cerqueira[23a], A. Cerri[29], L. Cerrito[75], F. Cerutti[47], S.A. Cetin[18b], F. Cevenini[102a,102b], A. Chafaq[135a], D. Chakraborty[106], K. Chan[2], B. Chapleau[85], J.D. Chapman[27], J.W. Chapman[87], E. Chareyre[78], D.G. Charlton[17], V. Chavda[82], S. Cheatham[85], S. Chekanov[5], S.V. Chekulaev[159a], G.A. Chelkov[65], M.A. Chelstowska[104], C. Chen[64], H. Chen[24], S. Chen[32c], T. Chen[32c], X. Chen[172], S. Cheng[32a], A. Cheplakov[65], V.F. Chepurnov[65], R. Cherkaoui El Moursli[135e], V. Chernyatin[24], E. Cheu[6], S.L. Cheung[158], L. Chevalier[136], G. Chiefari[102a,102b], L. Chikovani[51], J.T. Childers[58a], A. Chilingarov[71], G. Chiodini[72a], M.V. Chizhov[65], G. Choudalakis[30], S. Chouridou[137], I.A. Christidi[77], A. Christov[48], D. Chromek-Burckhart[29], M.L. Chu[151], J. Chudoba[125], G. Ciapetti[132a,132b], K. Ciba[37], A.K. Ciftci[3a], R. Ciftci[3a], D. Cinca[33], V. Cindro[74], M.D. Ciobotaru[163], C. Ciocca[19a,19b], A. Ciocio[14], M. Cirilli[87], M. Ciubancan[25a], A. Clark[49], P.J. Clark[45], W. Cleland[123], J.C. Clemens[83], B. Clement[55], C. Clement[146a,146b], R.W. Clifft[129], Y. Coadou[83], M. Cobal[164a,164c], A. Coccaro[50a,50b], J. Cochran[64], P. Coe[118], J.G. Cogan[143], J. Coggeshall[165], E. Cogneras[177], C.D. Cojocaru[28], J. Colas[4], A.P. Colijn[105], C. Collard[115], N.J. Collins[17], C. Collins-Tooth[53], J. Collot[55], G. Colon[84], P. Conde Muiño[124a], E. Coniavitis[118], M.C. Conidi[11], M. Consonni[104], V. Consorti[48], S. Constantinescu[25a], C. Conta[119a,119b], F. Conventi[102a,i], J. Cook[29], M. Cooke[14], B.D. Cooper[77], A.M. Cooper-Sarkar[118], N.J. Cooper-Smith[76], K. Copic[34], T. Cornelissen[50a,50b], M. Corradi[19a], F. Corriveau[85,j], A. Cortes-Gonzalez[165], G. Cortiana[99], G. Costa[89a], M.J. Costa[167], D. Costanzo[139], T. Costin[30], D. Côté[29], R. Coura Torres[23a], L. Courneyea[169], G. Cowan[76], C. Cowden[27], B.E. Cox[82], K. Cranmer[108], F. Crescioli[122a,122b], M. Cristinziani[20], G. Crosetti[36a,36b], R. Crupi[72a,72b], S. Crépé-Renaudin[55], C.-M. Cuciuc[25a], C. Cuenca Almenar[175], T. Cuhadar Donszelmann[139], S. Cuneo[50a,50b], M. Curatolo[47], C.J. Curtis[17], P. Cwetanski[61], H. Czirr[141], Z. Czyczula[117], S. D'Auria[53], M. D'Onofrio[73], A. D'Orazio[132a,132b], P.V.M. Da Silva[23a], C. Da Via[82], W. Dabrowski[37], T. Dai[87], C. Dallapiccola[84], M. Dam[35], M. Dameri[50a,50b], D.S. Damiani[137], H.O. Danielsson[29], D. Dannheim[99], V. Dao[49], G. Darbo[50a], G.L. Darlea[25b], C. Daum[105], J.P. Dauvergne[29], W. Davey[86], T. Davidek[126], N. Davidson[86], R. Davidson[71], E. Davies[118,c], M. Davies[93], A.R. Davison[77], Y. Davygora[58a], E. Dawe[142], I. Dawson[139], J.W. Dawson[5,*], R.K. Daya[39], K. De[7], R. de Asmundis[102a], S. De Castro[19a,19b], P.E. De Castro Faria Salgado[24], S. De Cecco[78], J. de Graat[98], N. De Groot[104], P. de Jong[105], C. De La Taille[115], H. De la Torre[80], B. De Lotto[164a,164c], L. De Mora[71], L. De Nooij[105], M. De Oliveira Branco[29], D. De Pedis[132a], P. de Saintignon[55], A. De Salvo[132a], U. De Sanctis[164a,164c], A. De Santo[149], J.B. De Vivie De Regie[115], S. Dean[77], D.V. Dedovich[65], J. Degenhardt[120], M. Dehchar[118], M. Deile[98], C. Del Papa[164a,164c], J. Del Peso[80], T. Del Prete[122a,122b], A. Dell'Acqua[29], L. Dell'Asta[89a,89b], M. Della Pietra[102a,i], D. della Volpe[102a,102b], M. Delmastro[29], P. Delpierre[83], N. Delruelle[29], P.A. Delsart[55], C. Deluca[148], S. Demers[175], M. Demichev[65], B. Demirkoz[11,k], J. Deng[163], S.P. Denisov[128], D. Derendarz[38], J.E. Derkaoui[135d], F. Derue[78], P. Dervan[73], K. Desch[20], E. Devetak[148], P.O. Deviveiros[158], A. Dewhurst[129], B. DeWilde[148], S. Dhaliwal[158], R. Dhullipudi[24,l], A. Di Ciaccio[133a,133b], L. Di Ciaccio[4], A. Di Girolamo[29], B. Di Girolamo[29], S. Di Luise[134a,134b], A. Di Mattia[88], B. Di Micco[29], R. Di Nardo[133a,133b], A. Di Simone[133a,133b], R. Di Sipio[19a,19b], M.A. Diaz[31a], F. Diblen[18c], E.B. Diehl[87], J. Dietrich[41], T.A. Dietzsch[58a], S. Diglio[115], K. Dindar Yagci[39], J. Dingfelder[20], C. Dionisi[132a,132b], P. Dita[25a], S. Dita[25a], F. Dittus[29], F. Djama[83], R. Djilkibaev[108], T. Djobava[51], M.A.B. do Vale[23a], A. Do Valle Wemans[124a], T.K.O. Doan[4], M. Dobbs[85], R. Dobinson[29,*], D. Dobos[42], E. Dobson[29], M. Dobson[163], J. Dodd[34], C. Doglioni[118], T. Doherty[53], Y. Doi[66,*], J. Dolejsi[126], I. Dolenc[74], Z. Dolezal[126], B.A. Dolgoshein[96,*], T. Dohmae[155], M. Donadelli[23b], M. Donega[120], J. Donini[55], J. Dopke[29], A. Doria[102a], A. Dos Anjos[172], M. Dosil[11], A. Dotti[122a,122b], M.T. Dova[70], J.D. Dowell[17], A.D. Doxiadis[105], A.T. Doyle[53], Z. Drasal[126], J. Drees[174], N. Dressnandt[120], H. Drevermann[29], C. Driouichi[35], M. Dris[9], J. Dubbert[99], T. Dubbs[137], S. Dube[14], E. Duchovni[171], G. Duckeck[98], A. Dudarev[29], F. Dudziak[64], M. Dührssen[29], I.P. Duerdoth[82], L. Duflot[115], M.-A. Dufour[85], M. Dunford[29], H. Duran Yildiz[3b], R. Duxfield[139], M. Dwuznik[37], F. Dydak[29], D. Dzahini[55], M. Düren[52], W.L. Ebenstein[44], J. Ebke[98], S. Eckert[48], S. Eckweiler[81], K. Edmonds[81], C.A. Edwards[76], N.C. Edwards[53], W. Ehrenfeld[41], T. Ehrich[99], T. Eifert[29], G. Eigen[13], K. Einsweiler[14], E. Eisenhandler[75], T. Ekelof[166], M. El Kacimi[135c], M. Ellert[166], S. Elles[4], F. Ellinghaus[81], K. Ellis[75], N. Ellis[29], J. Elmsheuser[98], M. Elsing[29], R. Ely[14], D. Emeliyanov[129], R. Engelmann[148], A. Engl[98], B. Epp[62], A. Eppig[87], J. Erdmann[54], A. Ereditato[16], D. Eriksson[146a], J. Ernst[1], M. Ernst[24], J. Ernwein[136], D. Errede[165], S. Errede[165], E. Ertel[81], M. Escalier[115], C. Escobar[167], X. Espinal Curull[11], B. Esposito[47], F. Etienne[83], A.I. Etienvre[136], E. Etzion[153], D. Evangelakou[54], H. Evans[61], L. Fabbri[19a,19b], C. Fabre[29], R.M. Fakhrutdinov[128], S. Falciano[132a], A.C. Falou[115], Y. Fang[172], M. Fanti[89a,89b], A. Farbin[7], A. Farilla[134a], J. Farley[148], T. Farooque[158], S.M. Farrington[118], P. Farthouat[29], P. Fassnacht[29], D. Fassouliotis[8], B. Fatholahzadeh[158], A. Favareto[89a,89b], L. Fayard[115], S. Fazio[36a,36b], R. Febbraro[33], P. Federic[144a], O.L. Fedin[121], W. Fedorko[88], M. Fehling-Kaschek[48], L. Feligioni[83], D. Fellmann[5], C.U. Felzmann[86], C. Feng[32d], E.J. Feng[30], A.B. Fenyuk[128], J. Ferencei[144b], J. Ferland[93], W. Fernando[109], S. Ferrag[53], J. Ferrando[53], V. Ferrara[41], A. Ferrari[166], P. Ferrari[105], R. Ferrari[119a], A. Ferrer[167], M.L. Ferrer[47], D. Ferrere[49], C. Ferretti[87], A. Ferretto Parodi[50a,50b], M. Fiascaris[30], F. Fiedler[81], A. Filipčič[74], A. Filippas[9], F. Filthaut[104], M. Fincke-Keeler[169], M.C.N. Fiolhais[124a,h], L. Fiorini[167], A. Firan[39], G. Fischer[41], P. Fischer[20], M.J. Fisher[109], S.M. Fisher[129], M. Flechl[48], I. Fleck[141], J. Fleckner[81], P. Fleischmann[173], S. Fleischmann[174], T. Flick[174], L.R. Flores Castillo[172], M.J. Flowerdew[99],

F. Föhlisch[58a], M. Fokitis[9], T. Fonseca Martin[16], D.A. Forbush[138], A. Formica[136], A. Forti[82], D. Fortin[159a], J.M. Foster[82], D. Fournier[115], A. Foussat[29], A.J. Fowler[44], K. Fowler[137], H. Fox[71], P. Francavilla[122a,122b], S. Franchino[119a,119b], D. Francis[29], T. Frank[171], M. Franklin[57], S. Franz[29], M. Fraternali[119a,119b], S. Fratina[120], S.T. French[27], R. Froeschl[29], D. Froidevaux[29], J.A. Frost[27], C. Fukunaga[156], E. Fullana Torregrosa[29], J. Fuster[167], C. Gabaldon[29], O. Gabizon[171], T. Gadfort[24], S. Gadomski[49], G. Gagliardi[50a,50b], P. Gagnon[61], C. Galea[98], E.J. Gallas[118], M.V. Gallas[29], V. Gallo[16], B.J. Gallop[129], P. Gallus[125], E. Galyaev[40], K.K. Gan[109], Y.S. Gao[143,f], V.A. Gapienko[128], A. Gaponenko[14], F. Garberson[175], M. Garcia-Sciveres[14], C. García[167], J.E. García Navarro[49], R.W. Gardner[30], N. Garelli[29], H. Garitaonandia[105], V. Garonne[29], J. Garvey[17], C. Gatti[47], G. Gaudio[119a], O. Gaumer[49], B. Gaur[141], L. Gauthier[136], I.L. Gavrilenko[94], C. Gay[168], G. Gaycken[20], J.-C. Gayde[29], E.N. Gazis[9], P. Ge[32d], C.N.P. Gee[129], D.A.A. Geerts[105], Ch. Geich-Gimbel[20], K. Gellerstedt[146a,146b], C. Gemme[50a], A. Gemmell[53], M.H. Genest[98], S. Gentile[132a,132b], M. George[54], S. George[76], P. Gerlach[174], A. Gershon[153], C. Geweniger[58a], H. Ghazlane[135b], P. Ghez[4], N. Ghodbane[33], B. Giacobbe[19a], S. Giagu[132a,132b], V. Giakoumopoulou[8], V. Giangiobbe[122a,122b], F. Gianotti[29], B. Gibbard[24], A. Gibson[158], S.M. Gibson[29], L.M. Gilbert[118], M. Gilchriese[14], V. Gilewsky[91], D. Gillberg[28], A.R. Gillman[129], D.M. Gingrich[2,e], J. Ginzburg[153], N. Giokaris[8], R. Giordano[102a,102b], F.M. Giorgi[15], P. Giovannini[99], P.F. Giraud[136], D. Giugni[89a], M. Giunta[132a,132b], P. Giusti[19a], B.K. Gjelsten[117], L.K. Gladilin[97], C. Glasman[80], J. Glatzer[48], A. Glazov[41], K.W. Glitza[174], G.L. Glonti[65], J. Godfrey[142], J. Godlewski[29], M. Goebel[41], T. Göpfert[43], C. Goeringer[81], C. Gössling[42], T. Göttfert[99], S. Goldfarb[87], D. Goldin[39], T. Golling[175], S.N. Golovnia[128], A. Gomes[124a,b], L.S. Gomez Fajardo[41], R. Gonçalo[76], J. Goncalves Pinto Firmino Da Costa[41], L. Gonella[20], A. Gonidec[29], S. Gonzalez[172], S. González de la Hoz[167], M.L. Gonzalez Silva[26], S. Gonzalez-Sevilla[49], J.J. Goodson[148], L. Goossens[29], P.A. Gorbounov[95], H.A. Gordon[24], I. Gorelov[103], G. Gorfine[174], B. Gorini[29], E. Gorini[72a,72b], A. Gorišek[74], E. Gornicki[38], S.A. Gorokhov[128], V.N. Goryachev[128], B. Gosdzik[41], M. Gosselink[105], M.I. Gostkin[65], M. Gouanère[4], I. Gough Eschrich[163], M. Gouighri[135a], D. Goujdami[135c], M.P. Goulette[49], A.G. Goussiou[138], C. Goy[4], I. Grabowska-Bold[163,g], V. Grabski[176], P. Grafström[29], C. Grah[174], K.-J. Grahn[41], F. Grancagnolo[72a], S. Grancagnolo[15], V. Grassi[148], V. Gratchev[121], N. Grau[34], H.M. Gray[29], J.A. Gray[148], E. Graziani[134a], O.G. Grebenyuk[121], D. Greenfield[129], T. Greenshaw[73], Z.D. Greenwood[24,l], I.M. Gregor[41], P. Grenier[143], J. Griffiths[138], N. Grigalashvili[65], A.A. Grillo[137], S. Grinstein[11], Y.V. Grishkevich[97], J.-F. Grivaz[115], J. Grognuz[29], M. Groh[99], E. Gross[171], J. Grosse-Knetter[54], J. Groth-Jensen[171], K. Grybel[141], V.J. Guarino[5], D. Guest[175], C. Guicheney[33], A. Guida[72a,72b], T. Guillemin[4], S. Guindon[54], H. Guler[85,m], J. Gunther[125], B. Guo[158], J. Guo[34], A. Gupta[30], Y. Gusakov[65], V.N. Gushchin[128], A. Gutierrez[93], P. Gutierrez[111], N. Guttman[153], O. Gutzwiller[172], C. Guyot[136], C. Gwenlan[118], C.B. Gwilliam[73], A. Haas[143], S. Haas[29], C. Haber[14], R. Hackenburg[24], H.K. Hadavand[39], D.R. Hadley[17], P. Haefner[99], F. Hahn[29], S. Haider[29], Z. Hajduk[38], H. Hakobyan[176], J. Haller[54], K. Hamacher[174], P. Hamal[113], A. Hamilton[49], S. Hamilton[161], H. Han[32a], L. Han[32b], K. Hanagaki[116], M. Hance[120], C. Handel[81], P. Hanke[58a], J.R. Hansen[35], J.B. Hansen[35], J.D. Hansen[35], P.H. Hansen[35], P. Hansson[143], K. Hara[160], G.A. Hare[137], T. Harenberg[174], S. Harkusha[90], D. Harper[87], R.D. Harrington[21], O.M. Harris[138], K. Harrison[17], J. Hartert[48], F. Hartjes[105], T. Haruyama[66], A. Harvey[56], S. Hasegawa[101], Y. Hasegawa[140], S. Hassani[136], M. Hatch[29], D. Hauff[99], S. Haug[16], M. Hauschild[29], R. Hauser[88], M. Havranek[20], B.M. Hawes[118], C.M. Hawkes[17], R.J. Hawkings[29], D. Hawkins[163], T. Hayakawa[67], D. Hayden[76], H.S. Hayward[73], S.J. Haywood[129], E. Hazen[21], M. He[32d], S.J. Head[17], V. Hedberg[79], L. Heelan[7], S. Heim[88], B. Heinemann[14], S. Heisterkamp[35], L. Helary[4], M. Heller[115], S. Hellman[146a,146b], C. Helsens[11], R.C.W. Henderson[71], M. Henke[58a], A. Henrichs[54], A.M. Henriques Correia[29], S. Henrot-Versille[115], F. Henry-Couannier[83], C. Hensel[54], T. Henß[174], C.M. Hernandez[7], Y. Hernández Jiménez[167], R. Herrberg[15], A.D. Hershenhorn[152], G. Herten[48], R. Hertenberger[98], L. Hervas[29], N.P. Hessey[105], A. Hidvegi[146a], E. Higón-Rodriguez[167], D. Hill[5,*], J.C. Hill[27], N. Hill[5], K.H. Hiller[41], S. Hillert[20], S.J. Hillier[17], I. Hinchliffe[14], E. Hines[120], M. Hirose[116], F. Hirsch[42], D. Hirschbuehl[174], J. Hobbs[148], N. Hod[153], M.C. Hodgkinson[139], P. Hodgson[139], A. Hoecker[29], M.R. Hoeferkamp[103], J. Hoffman[39], D. Hoffmann[83], M. Hohlfeld[81], M. Holder[141], A. Holmes[118], S.O. Holmgren[146a], A. Holtsch[41], T. Holy[127], J.L. Holzbauer[88], Y. Homma[67], T.M. Hong[120], L. Hooft van Huysduynen[108], T. Horazdovsky[127], C. Horn[143], S. Horner[48], K. Horton[118], J.-Y. Hostachy[55], S. Hou[151], M.A. Houlden[73], A. Hoummada[135a], J. Howarth[82], D.F. Howell[118], I. Hristova[15], J. Hrivnac[115], I. Hruska[125], T. Hryn'ova[4], P.J. Hsu[175], S.-C. Hsu[14], G.S. Huang[111], Z. Hubacek[127], F. Hubaut[83], F. Huegging[20], T.B. Huffman[118], E.W. Hughes[34], G. Hughes[71], R.E. Hughes-Jones[82], M. Huhtinen[29], P. Hurst[57], M. Hurwitz[14], U. Husemann[41], N. Huseynov[65,n], J. Huston[88], J. Huth[57], G. Iacobucci[49], G. Iakovidis[9], M. Ibbotson[82], I. Ibragimov[141], R. Ichimiya[67], L. Iconomidou-Fayard[115], J. Idarraga[115], M. Idzik[37], P. Iengo[102a,102b], O. Igonkina[105], Y. Ikegami[66], M. Ikeno[66], Y. Ilchenko[39], D. Iliadis[154], D. Imbault[78], M. Imhaeuser[174], M. Imori[155], T. Ince[20], J. Inigo-Golfin[29], P. Ioannou[8], M. Iodice[134a], G. Ionescu[4], A. Irles Quiles[167], K. Ishii[66], A. Ishikawa[67], M. Ishino[66], R. Ishmukhametov[39], C. Issever[118], S. Istin[18a], Y. Itoh[101], A.V. Ivashin[128], W. Iwanski[38], H. Iwasaki[66], J.M. Izen[40], V. Izzo[102a], B. Jackson[120], J.N. Jackson[73], P. Jackson[143], M.R. Jaekel[29], V. Jain[61], K. Jakobs[48], S. Jakobsen[35], J. Jakubek[127], D.K. Jana[111], E. Jankowski[158], E. Jansen[77], A. Jantsch[99], M. Janus[20], G. Jarlskog[79], L. Jeanty[57], K. Jelen[37], I. Jen-La Plante[30], P. Jenni[29], A. Jeremie[4], P. Jež[35], S. Jézéquel[4], M.K. Jha[19a],

H. Ji[172], W. Ji[81], J. Jia[148], Y. Jiang[32b], M. Jimenez Belenguer[41], G. Jin[32b], S. Jin[32a], O. Jinnouchi[157], M.D. Joergensen[35], D. Joffe[39], L.G. Johansen[13], M. Johansen[146a,146b], K.E. Johansson[146a], P. Johansson[139], S. Johnert[41], K.A. Johns[6], K. Jon-And[146a,146b], G. Jones[82], R.W.L. Jones[71], T.W. Jones[77], T.J. Jones[73], O. Jonsson[29], C. Joram[29], P.M. Jorge[124a,b], J. Joseph[14], X. Ju[130], V. Juranek[125], P. Jussel[62], V.V. Kabachenko[128], S. Kabana[16], M. Kaci[167], A. Kaczmarska[38], P. Kadlecik[35], M. Kado[115], H. Kagan[109], M. Kagan[57], S. Kaiser[99], E. Kajomovitz[152], S. Kalinin[174], L.V. Kalinovskaya[65], S. Kama[39], N. Kanaya[155], M. Kaneda[29], T. Kanno[157], V.A. Kantserov[96], J. Kanzaki[66], B. Kaplan[175], A. Kapliy[30], J. Kaplon[29], D. Kar[43], M. Karagoz[118], M. Karnevskiy[41], K. Karr[5], V. Kartvelishvili[71], A.N. Karyukhin[128], L. Kashif[172], A. Kasmi[39], R.D. Kass[109], A. Kastanas[13], M. Kataoka[4], Y. Kataoka[155], E. Katsoufis[9], J. Katzy[41], V. Kaushik[6], K. Kawagoe[67], T. Kawamoto[155], G. Kawamura[81], M.S. Kayl[105], V.A. Kazanin[107], M.Y. Kazarinov[65], J.R. Keates[82], R. Keeler[169], R. Kehoe[39], M. Keil[54], G.D. Kekelidze[65], M. Kelly[82], J. Kennedy[98], C.J. Kenney[143], M. Kenyon[53], O. Kepka[125], N. Kerschen[29], B.P. Kerševan[74], S. Kersten[174], K. Kessoku[155], C. Ketterer[48], J. Keung[158], M. Khakzad[28], F. Khalil-zada[10], H. Khandanyan[165], A. Khanov[112], D. Kharchenko[65], A. Khodinov[96], A.G. Kholodenko[128], A. Khomich[58a], T.J. Khoo[27], G. Khoriauli[20], A. Khoroshilov[174], N. Khovanskiy[65], V. Khovanskiy[95], E. Khramov[65], J. Khubua[51], H. Kim[7], M.S. Kim[2], P.C. Kim[143], S.H. Kim[160], N. Kimura[170], O. Kind[15], B.T. King[73], M. King[67], R.S.B. King[118], J. Kirk[129], G.P. Kirsch[118], L.E. Kirsch[22], A.E. Kiryunin[99], D. Kisielewska[37], T. Kittelmann[123], A.M. Kiver[128], H. Kiyamura[67], E. Kladiva[144b], J. Klaiber-Lodewigs[42], M. Klein[73], U. Klein[73], K. Kleinknecht[81], M. Klemetti[85], A. Klier[171], A. Klimentov[24], R. Klingenberg[42], E.B. Klinkby[35], T. Klioutchnikova[29], P.F. Klok[104], S. Klous[105], E.-E. Kluge[58a], T. Kluge[73], P. Kluit[105], S. Kluth[99], E. Kneringer[62], J. Knobloch[29], E.B.F.G. Knoops[83], A. Knue[54], B.R. Ko[44], T. Kobayashi[155], M. Kobel[43], M. Kocian[143], A. Kocnar[113], P. Kodys[126], K. Köneke[29], A.C. König[104], S. Koenig[81], L. Köpke[81], F. Koetsveld[104], P. Koevesarki[20], T. Koffas[29], E. Koffeman[105], F. Kohn[54], Z. Kohout[127], T. Kohriki[66], T. Koi[143], T. Kokott[20], G.M. Kolachev[107], H. Kolanoski[15], V. Kolesnikov[65], I. Koletsou[89a], J. Koll[88], D. Kollar[29], M. Kollefrath[48], S.D. Kolya[82], A.A. Komar[94], J.R. Komaragiri[142], Y. Komori[155], T. Kondo[66], T. Kono[41,o], A.I. Kononov[48], R. Konoplich[108,p], N. Konstantinidis[77], A. Kootz[174], S. Koperny[37], S.V. Kopikov[128], K. Korcyl[38], K. Kordas[154], V. Koreshev[128], A. Korn[14], A. Korol[107], I. Korolkov[11], E.V. Korolkova[139], V.A. Korotkov[128], O. Kortner[99], S. Kortner[99], V.V. Kostyukhin[20], M.J. Kotamäki[29], S. Kotov[99], V.M. Kotov[65], A. Kotwal[44], C. Kourkoumelis[8], V. Kouskoura[154], A. Koutsman[105], R. Kowalewski[169], T.Z. Kowalski[37], W. Kozanecki[136], A.S. Kozhin[128], V. Kral[127], V.A. Kramarenko[97], G. Kramberger[74], O. Krasel[42], M.W. Krasny[78], A. Krasznahorkay[108], J. Kraus[88], A. Kreisel[153], F. Krejci[127], J. Kretzschmar[73], N. Krieger[54], P. Krieger[158], K. Kroeninger[54], H. Kroha[99], J. Kroll[120], J. Kroseberg[20], J. Krstic[12a], U. Kruchonak[65], H. Krüger[20], T. Kruker[16], Z.V. Krumshteyn[65], A. Kruth[20], T. Kubota[86], S. Kuehn[48], A. Kugel[58c], T. Kuhl[174], D. Kuhn[62], V. Kukhtin[65], Y. Kulchitsky[90], S. Kuleshov[31b], C. Kummer[98], M. Kuna[78], N. Kundu[118], J. Kunkle[120], A. Kupco[125], H. Kurashige[67], M. Kurata[160], Y.A. Kurochkin[90], V. Kus[125], W. Kuykendall[138], M. Kuze[157], P. Kuzhir[91], O. Kvasnicka[125], J. Kvita[29], R. Kwee[15], A. La Rosa[172], L. La Rotonda[36a,36b], L. Labarga[80], J. Labbe[4], S. Lablak[135a], C. Lacasta[167], F. Lacava[132a,132b], H. Lacker[15], D. Lacour[78], V.R. Lacuesta[167], E. Ladygin[65], R. Lafaye[4], B. Laforge[78], T. Lagouri[80], S. Lai[48], E. Laisne[55], M. Lamanna[29], C.L. Lampen[6], W. Lampl[6], E. Lancon[136], U. Landgraf[48], M.P.J. Landon[75], H. Landsman[152], J.L. Lane[82], C. Lange[41], A.J. Lankford[163], F. Lanni[24], K. Lantzsch[29], S. Laplace[78], C. Lapoire[20], J.F. Laporte[136], T. Lari[89a], A.V. Larionov[128], A. Larner[118], C. Lasseur[29], M. Lassnig[29], W. Lau[118], P. Laurelli[47], A. Lavorato[118], W. Lavrijsen[14], P. Laycock[73], A.B. Lazarev[65], A. Lazzaro[89a,89b], O. Le Dortz[78], E. Le Guirriec[83], C. Le Maner[158], E. Le Menedeu[136], A. Lebedev[64], C. Lebel[93], T. LeCompte[5], F. Ledroit-Guillon[55], H. Lee[105], J.S.H. Lee[150], S.C. Lee[151], L. Lee[175], M. Lefebvre[169], M. Legendre[136], A. Leger[49], B.C. LeGeyt[120], F. Legger[98], C. Leggett[14], M. Lehmacher[20], G. Lehmann Miotto[29], X. Lei[6], M.A.L. Leite[23b], R. Leitner[126], D. Lellouch[171], J. Lellouch[78], M. Leltchouk[34], V. Lendermann[58a], K.J.C. Leney[145b], T. Lenz[174], G. Lenzen[174], B. Lenzi[29], K. Leonhardt[43], S. Leontsinis[9], C. Leroy[93], J.-R. Lessard[169], J. Lesser[146a], C.G. Lester[27], A. Leung Fook Cheong[172], J. Levêque[4], D. Levin[87], L.J. Levinson[171], M.S. Levitski[128], M. Lewandowska[21], A. Lewis[118], G.H. Lewis[108], A.M. Leyko[20], M. Leyton[15], B. Li[83], H. Li[172], S. Li[32b,d], X. Li[87], Z. Liang[39], Z. Liang[118,q], B. Liberti[133a], P. Lichard[29], M. Lichtnecker[98], K. Lie[165], W. Liebig[13], R. Lifshitz[152], J.N. Lilley[17], C. Limbach[20], A. Limosani[86], M. Limper[63], S.C. Lin[151,r], F. Linde[105], J.T. Linnemann[88], E. Lipeles[120], L. Lipinsky[125], A. Lipniacka[13], T.M. Liss[165], D. Lissauer[24], A. Lister[49], A.M. Litke[137], C. Liu[28], D. Liu[151,s], H. Liu[87], J.B. Liu[87], M. Liu[32b], S. Liu[2], Y. Liu[32b], M. Livan[119a,119b], S.S.A. Livermore[118], A. Lleres[55], J. Llorente Merino[80], S.L. Lloyd[75], E. Lobodzinska[41], P. Loch[6], W.S. Lockman[137], S. Lockwitz[175], T. Loddenkoetter[20], F.K. Loebinger[82], A. Loginov[175], C.W. Loh[168], T. Lohse[15], K. Lohwasser[48], M. Lokajicek[125], J. Loken[118], V.P. Lombardo[4], R.E. Long[71], L. Lopes[124a,b], D. Lopez Mateos[34,t], M. Losada[162], P. Loscutoff[14], F. Lo Sterzo[132a,132b], M.J. Losty[159a], X. Lou[40], A. Lounis[115], K.F. Loureiro[162], J. Love[21], P.A. Love[71], A.J. Lowe[143,f], F. Lu[32a], H.J. Lubatti[138], C. Luci[132a,132b], A. Lucotte[55], A. Ludwig[43], D. Ludwig[41], I. Ludwig[48], J. Ludwig[48], F. Luehring[61], G. Luijckx[105], D. Lumb[48], L. Luminari[132a], E. Lund[117], B. Lund-Jensen[147], B. Lundberg[79], J. Lundberg[146a,146b], J. Lundquist[35], M. Lungwitz[81], A. Lupi[122a,122b], G. Lutz[99], D. Lynn[24], J. Lys[14], E. Lytken[79], H. Ma[24], L.L. Ma[172], J.A. Macana Goia[93], G. Maccarrone[47], A. Macchiolo[99], B. Maček[74], J. Machado Miguens[124a], D. Macina[49], R. Mackeprang[35], R.J. Madaras[14], W.F. Mader[43], R. Maenner[58c],

T. Maeno[24], P. Mättig[174], S. Mättig[41], P.J. Magalhaes Martins[124a,h], L. Magnoni[29], E. Magradze[54], Y. Mahalalel[153], K. Mahboubi[48], G. Mahout[17], C. Maiani[132a,132b], C. Maidantchik[23a], A. Maio[124a,b], S. Majewski[24], Y. Makida[66], N. Makovec[115], P. Mal[6], Pa. Malecki[38], P. Malecki[38], V.P. Maleev[121], F. Malek[55], U. Mallik[63], D. Malon[5], S. Maltezos[9], V. Malyshev[107], S. Malyukov[29], R. Mameghani[98], J. Mamuzic[12b], A. Manabe[66], L. Mandelli[89a], I. Mandić[74], R. Mandrysch[15], J. Maneira[124a], P.S. Mangeard[88], I.D. Manjavidze[65], A. Mann[54], P.M. Manning[137], A. Manousakis-Katsikakis[8], B. Mansoulie[136], A. Manz[99], A. Mapelli[29], L. Mapelli[29], L. March[80], J.F. Marchand[29], F. Marchese[133a,133b], G. Marchiori[78], M. Marcisovsky[125], A. Marin[21,*], C.P. Marino[61], F. Marroquim[23a], R. Marshall[82], Z. Marshall[29], F.K. Martens[158], S. Marti-Garcia[167], A.J. Martin[175], B. Martin[29], B. Martin[88], F.F. Martin[120], J.P. Martin[93], Ph. Martin[55], T.A. Martin[17], B. Martin dit Latour[49], M. Martinez[11], V. Martinez Outschoorn[57], A.C. Martyniuk[82], M. Marx[82], F. Marzano[132a], A. Marzin[111], L. Masetti[81], T. Mashimo[155], R. Mashinistov[94], J. Masik[82], A.L. Maslennikov[107], M. Maß[42], I. Massa[19a,19b], G. Massaro[105], N. Massol[4], P. Mastrandrea[132a,132b], A. Mastroberardino[36a,36b], T. Masubuchi[155], M. Mathes[20], P. Matricon[115], H. Matsumoto[155], H. Matsunaga[155], T. Matsushita[67], C. Mattravers[118,c], J.M. Maugain[29], S.J. Maxfield[73], D.A. Maximov[107], E.N. May[5], A. Mayne[139], R. Mazini[151], M. Mazur[20], M. Mazzanti[89a], E. Mazzoni[122a,122b], S.P. Mc Kee[87], A. McCarn[165], R.L. McCarthy[148], T.G. McCarthy[28], N.A. McCubbin[129], K.W. McFarlane[56], J.A. Mcfayden[139], H. McGlone[53], G. Mchedlidze[51], R.A. McLaren[29], T. Mclaughlan[17], S.J. McMahon[129], R.A. McPherson[169,j], A. Meade[84], J. Mechnich[105], M. Mechtel[174], M. Medinnis[41], R. Meera-Lebbai[111], T. Meguro[116], R. Mehdiyev[93], S. Mehlhase[35], A. Mehta[73], K. Meier[58a], J. Meinhardt[48], B. Meirose[79], C. Melachrinos[30], B.R. Mellado Garcia[172], L. Mendoza Navas[162], Z. Meng[151,s], A. Mengarelli[19a,19b], S. Menke[99], C. Menot[29], E. Meoni[11], K.M. Mercurio[57], P. Mermod[118], L. Merola[102a,102b], C. Meroni[89a], F.S. Merritt[30], A. Messina[29], J. Metcalfe[103], A.S. Mete[64], S. Meuser[20], C. Meyer[81], J.-P. Meyer[136], J. Meyer[173], J. Meyer[54], T.C. Meyer[29], W.T. Meyer[64], J. Miao[32d], S. Michal[29], L. Micu[25a], R.P. Middleton[129], P. Miele[29], S. Migas[73], L. Mijović[41], G. Mikenberg[171], M. Mikestikova[125], M. Mikuž[74], D.W. Miller[143], R.J. Miller[88], W.J. Mills[168], C. Mills[57], A. Milov[171], D.A. Milstead[146a,146b], D. Milstein[171], A.A. Minaenko[128], M. Miñano[167], I.A. Minashvili[65], A.I. Mincer[108], B. Mindur[37], M. Mineev[65], Y. Ming[130], L.M. Mir[11], G. Mirabelli[132a], L. Miralles Verge[11], A. Misiejuk[76], J. Mitrevski[137], G.Y. Mitrofanov[128], V.A. Mitsou[167], S. Mitsui[66], P.S. Miyagawa[82], K. Miyazaki[67], J.U. Mjörnmark[79], T. Moa[146a,146b], P. Mockett[138], S. Moed[57], V. Moeller[27], K. Mönig[41], N. Möser[20], S. Mohapatra[148], B. Mohn[13], W. Mohr[48], S. Mohrdieck-Möck[99], A.M. Moisseev[128,*], R. Moles-Valls[167], J. Molina-Perez[29], J. Monk[77], E. Monnier[83], S. Montesano[89a,89b], F. Monticelli[70], S. Monzani[19a,19b], R.W. Moore[2], G.F. Moorhead[86], C. Mora Herrera[49], A. Moraes[53], A. Morais[124a,b], N. Morange[136], J. Morel[54], G. Morello[36a,36b], D. Moreno[81], M. Moreno Llácer[167], P. Morettini[50a], M. Morii[57], J. Morin[75], Y. Morita[66], A.K. Morley[29], G. Mornacchi[29], M.-C. Morone[49], S.V. Morozov[96], J.D. Morris[75], L. Morvaj[101], H.G. Moser[99], M. Mosidze[51], J. Moss[109], R. Mount[143], E. Mountricha[136], S.V. Mouraviev[94], E.J.W. Moyse[84], M. Mudrinic[12b], F. Mueller[58a], J. Mueller[123], K. Mueller[20], T.A. Müller[98], D. Muenstermann[29], A. Muijs[105], A. Muir[168], Y. Munwes[153], K. Murakami[66], W.J. Murray[129], I. Mussche[105], E. Musto[102a,102b], A.G. Myagkov[128], M. Myska[125], J. Nadal[11], K. Nagai[160], K. Nagano[66], Y. Nagasaka[60], A.M. Nairz[29], Y. Nakahama[29], K. Nakamura[155], I. Nakano[110], G. Nanava[20], A. Napier[161], M. Nash[77,c], N.R. Nation[21], T. Nattermann[20], T. Naumann[41], G. Navarro[162], H.A. Neal[87], E. Nebot[80], P.Yu. Nechaeva[94], A. Negri[119a,119b], G. Negri[29], S. Nektarijevic[49], A. Nelson[64], S. Nelson[143], T.K. Nelson[143], S. Nemecek[125], P. Nemethy[108], A.A. Nepomuceno[23a], M. Nessi[29,u], S.Y. Nesterov[121], M.S. Neubauer[165], A. Neusiedl[81], R.M. Neves[108], P. Nevski[24], P.R. Newman[17], V. Nguyen Thi Hong[136], R.B. Nickerson[118], R. Nicolaidou[136], L. Nicolas[139], B. Nicquevert[29], F. Niedercorn[115], J. Nielsen[137], T. Niinikoski[29], A. Nikiforov[15], V. Nikolaenko[128], K. Nikolaev[65], I. Nikolic-Audit[78], K. Nikolopoulos[24], H. Nilsen[48], P. Nilsson[7], Y. Ninomiya[155], A. Nisati[132a], T. Nishiyama[67], R. Nisius[99], L. Nodulman[5], M. Nomachi[116], I. Nomidis[154], M. Nordberg[29], B. Nordkvist[146a,146b], P.R. Norton[129], J. Novakova[126], M. Nozaki[66], M. Nožička[41], L. Nozka[113], I.M. Nugent[159a], A.-E. Nuncio-Quiroz[20], G. Nunes Hanninger[20], T. Nunnemann[98], E. Nurse[77], T. Nyman[29], B.J. O'Brien[45], S.W. O'Neale[17,*], D.C. O'Neil[142], V. O'Shea[53], F.G. Oakham[28,e], H. Oberlack[99], J. Ocariz[78], A. Ochi[67], S. Oda[155], S. Odaka[66], J. Odier[83], H. Ogren[61], A. Oh[82], S.H. Oh[44], C.C. Ohm[146a,146b], T. Ohshima[101], H. Ohshita[140], T.K. Ohska[66], T. Ohsugi[59], S. Okada[67], H. Okawa[163], Y. Okumura[101], T. Okuyama[155], M. Olcese[50a], A.G. Olchevski[65], M. Oliveira[124a,h], D. Oliveira Damazio[24], E. Oliver Garcia[167], D. Olivito[120], A. Olszewski[38], J. Olszowska[38], C. Omachi[67], A. Onofre[124a,v], P.U.E. Onyisi[30], C.J. Oram[159a], M.J. Oreglia[30], Y. Oren[153], D. Orestano[134a,134b], I. Orlov[107], C. Oropeza Barrera[53], R.S. Orr[158], E.O. Ortega[130], B. Osculati[50a,50b], R. Ospanov[120], C. Osuna[11], G. Otero y Garzon[26], J.P. Ottersbach[105], M. Ouchrif[135d], F. Ould-Saada[117], A. Ouraou[136], Q. Ouyang[32a], M. Owen[82], S. Owen[139], O.K. Øye[13], V.E. Ozcan[18a], N. Ozturk[7], A. Pacheco Pages[11], C. Padilla Aranda[11], E. Paganis[139], F. Paige[24], K. Pajchel[117], S. Palestini[29], D. Pallin[33], A. Palma[124a,b], J.D. Palmer[17], Y.B. Pan[172], E. Panagiotopoulou[9], B. Panes[31a], N. Panikashvili[87], S. Panitkin[24], D. Pantea[25a], M. Panuskova[125], V. Paolone[123], A. Papadelis[146a], Th.D. Papadopoulou[9], A. Paramonov[5], W. Park[24,w], M.A. Parker[27], F. Parodi[50a,50b], J.A. Parsons[34], U. Parzefall[48], E. Pasqualucci[132a], A. Passeri[134a], F. Pastore[134a,134b], Fr. Pastore[29], G. Pásztor[49,x], S. Pataraia[172], N. Patel[150], J.R. Pater[82], S. Patricelli[102a,102b], T. Pauly[29],

M. Pecsy[144a], M.I. Pedraza Morales[172], S.V. Peleganchuk[107], H. Peng[172], R. Pengo[29], A. Penson[34], J. Penwell[61], M. Perantoni[23a], K. Perez[34,t], T. Perez Cavalcanti[41], E. Perez Codina[11], M.T. Pérez García-Estañ[167], V. Perez Reale[34], L. Perini[89a,89b], H. Pernegger[29], R. Perrino[72a], P. Perrodo[4], S. Persembe[3a], V.D. Peshekhonov[65], O. Peters[105], B.A. Petersen[29], J. Petersen[29], T.C. Petersen[35], E. Petit[83], A. Petridis[154], C. Petridou[154], E. Petrolo[132a], F. Petrucci[134a,134b], D. Petschull[41], M. Petteni[142], R. Pezoa[31b], A. Phan[86], A.W. Phillips[27], P.W. Phillips[129], G. Piacquadio[29], E. Piccaro[75], M. Piccinini[19a,19b], A. Pickford[53], S.M. Piec[41], R. Piegaia[26], J.E. Pilcher[30], A.D. Pilkington[82], J. Pina[124a,b], M. Pinamonti[164a,164c], A. Pinder[118], J.L. Pinfold[2], J. Ping[32c], B. Pinto[124a,b], O. Pirotte[29], C. Pizio[89a,89b], R. Placakyte[41], M. Plamondon[169], W.G. Plano[82], M.-A. Pleier[24], A.V. Pleskach[128], A. Poblaguev[24], S. Poddar[58a], F. Podlyski[33], L. Poggioli[115], T. Poghosyan[20], M. Pohl[49], F. Polci[55], G. Polesello[119a], A. Policicchio[138], A. Polini[19a], J. Poll[75], V. Polychronakos[24], D.M. Pomarede[136], D. Pomeroy[22], K. Pommès[29], L. Pontecorvo[132a], B.G. Pope[88], G.A. Popeneciu[25a], D.S. Popovic[12a], A. Poppleton[29], R. Porter[163], C. Posch[21], G.E. Pospelov[99], S. Pospisil[127], I.N. Potrap[99], C.J. Potter[149], C.T. Potter[114], G. Poulard[29], J. Poveda[172], R. Prabhu[77], P. Pralavorio[83], S. Prasad[57], R. Pravahan[7], S. Prell[64], K. Pretzl[16], L. Pribyl[29], D. Price[61], L.E. Price[5], M.J. Price[29], P.M. Prichard[73], D. Prieur[123], M. Primavera[72a], K. Prokofiev[108], F. Prokoshin[31b], S. Protopopescu[24], J. Proudfoot[5], X. Prudent[43], H. Przysiezniak[4], S. Psoroulas[20], E. Ptacek[114], J. Purdham[87], M. Purohit[24,w], P. Puzo[115], Y. Pylypchenko[117], J. Qian[87], Z. Qian[83], Z. Qin[41], A. Quadt[54], D.R. Quarrie[14], W.B. Quayle[172], F. Quinonez[31a], M. Raas[104], V. Radescu[58b], B. Radics[20], T. Rador[18a], F. Ragusa[89a,89b], G. Rahal[177], A.M. Rahimi[109], D. Rahm[24], S. Rajagopalan[24], M. Rammensee[48], M. Rammes[141], M. Ramstedt[146a,146b], K. Randrianarivony[28], P.N. Ratoff[71], F. Rauscher[98], E. Rauter[99], M. Raymond[29], A.L. Read[117], D.M. Rebuzzi[119a,119b], A. Redelbach[173], G. Redlinger[24], R. Reece[120], K. Reeves[40], A. Reichold[105], E. Reinherz-Aronis[153], A. Reinsch[114], I. Reisinger[42], D. Reljic[12a], C. Rembser[29], Z.L. Ren[151], A. Renaud[115], P. Renkel[39], M. Rescigno[132a], S. Resconi[89a], B. Resende[136], P. Reznicek[98], R. Rezvani[158], A. Richards[77], R. Richter[99], E. Richter-Was[38,y], M. Ridel[78], S. Rieke[81], M. Rijpstra[105], M. Rijssenbeek[148], A. Rimoldi[119a,119b], L. Rinaldi[19a], R.R. Rios[39], I. Riu[11], G. Rivoltella[89a,89b], F. Rizatdinova[112], E. Rizvi[75], S.H. Robertson[85,j], A. Robichaud-Veronneau[49], D. Robinson[27], J.E.M. Robinson[77], M. Robinson[114], A. Robson[53], J.G. Rocha de Lima[106], C. Roda[122a,122b], D. Roda Dos Santos[29], S. Rodier[80], D. Rodriguez[162], Y. Rodriguez Garcia[15], A. Roe[54], S. Roe[29], O. Røhne[117], V. Rojo[1], S. Rolli[161], A. Romaniouk[96], V.M. Romanov[65], G. Romeo[26], D. Romero Maltrana[31a], L. Roos[78], E. Ros[167], S. Rosati[132a,132b], K. Rosbach[49], M. Rose[76], G.A. Rosenbaum[158], E.I. Rosenberg[64], P.L. Rosendahl[13], L. Rosselet[49], V. Rossetti[11], E. Rossi[102a,102b], L.P. Rossi[50a], L. Rossi[89a,89b], M. Rotaru[25a], I. Roth[171], J. Rothberg[138], D. Rousseau[115], C.R. Royon[136], A. Rozanov[83], Y. Rozen[152], X. Ruan[115], I. Rubinskiy[41], B. Ruckert[98], N. Ruckstuhl[105], V.I. Rud[97], G. Rudolph[62], F. Rühr[6], F. Ruggieri[134a,134b], A. Ruiz-Martinez[64], E. Rulikowska-Zarebska[37], V. Rumiantsev[91,*], L. Rumyantsev[65], K. Runge[48], O. Runolfsson[20], Z. Rurikova[48], N.A. Rusakovich[65], D.R. Rust[61], J.P. Rutherfoord[6], C. Ruwiedel[14], P. Ruzicka[125], Y.F. Ryabov[121], V. Ryadovikov[128], P. Ryan[88], M. Rybar[126], G. Rybkin[115], N.C. Ryder[118], S. Rzaeva[10], A.F. Saavedra[150], I. Sadeh[153], H.F.-W. Sadrozinski[137], R. Sadykov[65], F. Safai Tehrani[132a,132b], H. Sakamoto[155], G. Salamanna[75], A. Salamon[133a], M. Saleem[111], D. Salihagic[99], A. Salnikov[143], J. Salt[167], B.M. Salvachua Ferrando[5], D. Salvatore[36a,36b], F. Salvatore[149], A. Salvucci[104], A. Salzburger[29], D. Sampsonidis[154], B.H. Samset[117], H. Sandaker[13], H.G. Sander[81], M.P. Sanders[98], M. Sandhoff[174], T. Sandoval[27], R. Sandstroem[99], S. Sandvoss[174], D.P.C. Sankey[129], A. Sansoni[47], C. Santamarina Rios[85], C. Santoni[33], R. Santonico[133a,133b], H. Santos[124a], J.G. Saraiva[124a,b], T. Sarangi[172], E. Sarkisyan-Grinbaum[7], F. Sarri[122a,122b], G. Sartisohn[174], O. Sasaki[66], T. Sasaki[66], N. Sasao[68], I. Satsounkevitch[90], G. Sauvage[4], J.B. Sauvan[115], P. Savard[158,e], V. Savinov[123], D.O. Savu[29], P. Savva[9], L. Sawyer[24,l], D.H. Saxon[53], L.P. Says[33], C. Sbarra[19a,19b], A. Sbrizzi[19a,19b], O. Scallon[93], D.A. Scannicchio[163], J. Schaarschmidt[115], P. Schacht[99], U. Schäfer[81], S. Schaepe[20], S. Schaetzel[58b], A.C. Schaffer[115], D. Schaile[98], R.D. Schamberger[148], A.G. Schamov[107], V. Scharf[58a], V.A. Schegelsky[121], D. Scheirich[87], M. Schernau[163], M.I. Scherzer[14], C. Schiavi[50a,50b], J. Schieck[98], M. Schioppa[36a,36b], S. Schlenker[29], J.L. Schlereth[5], E. Schmidt[48], K. Schmieden[20], C. Schmitt[81], S. Schmitt[58b], M. Schmitz[20], M. Schneider[41], A. Schöning[58b], M. Schott[29], D. Schouten[142], J. Schovancova[125], M. Schram[85], C. Schroeder[81], N. Schroer[58c], S. Schuh[29], G. Schuler[29], J. Schultes[174], H.-C. Schultz-Coulon[58a], H. Schulz[15], J.W. Schumacher[20], M. Schumacher[48], B.A. Schumm[137], Ph. Schune[136], C. Schwanenberger[82], A. Schwartzman[143], Ph. Schwemling[78], R. Schwienhorst[88], R. Schwierz[43], J. Schwindling[136], W.G. Scott[129], J. Searcy[114], E. Sedykh[121], E. Segura[11], S.C. Seidel[103], A. Seiden[137], F. Seifert[43], J.M. Seixas[23a], G. Sekhniaidze[102a], D.M. Seliverstov[121], B. Sellden[146a], G. Sellers[73], M. Seman[144b], N. Semprini-Cesari[19a,19b], C. Serfon[98], L. Serin[115], R. Seuster[99], H. Severini[111], M.E. Sevior[86], A. Sfyrla[29], E. Shabalina[54], M. Shamim[114], L.Y. Shan[32a], J.T. Shank[21], Q.T. Shao[86], M. Shapiro[14], P.B. Shatalov[95], L. Shaver[6], C. Shaw[53], K. Shaw[164a,164c], D. Sherman[175], P. Sherwood[77], A. Shibata[108], H. Shichi[101], S. Shimizu[29], M. Shimojima[100], T. Shin[56], A. Shmeleva[94], M.J. Shochet[30], D. Short[118], M.A. Shupe[6], P. Sicho[125], A. Sidoti[132a,132b], A. Siebel[174], F. Siegert[48], J. Siegrist[14], Dj. Sijacki[12a], O. Silbert[171], J. Silva[124a,b], Y. Silver[153], D. Silverstein[143], S.B. Silverstein[146a], V. Simak[127], O. Simard[136], Lj. Simic[12a], S. Simion[115], B. Simmons[77], M. Simonyan[35], P. Sinervo[158], N.B. Sinev[114], V. Sipica[141], G. Siragusa[173], A.N. Sisakyan[65], S.Yu. Sivoklokov[97], J. Sjölin[146a,146b], T.B. Sjursen[13], L.A. Skinnari[14], K. Skovpen[107], P. Skubic[111], N. Skvorodnev[22], M. Slater[17], T. Slavicek[127], K. Sliwa[161], T.J. Sloan[71], J. Sloper[29], V. Smakhtin[171], S.Yu. Smirnov[96], L.N. Smirnova[97], O. Smirnova[79], B.C. Smith[57], D. Smith[143], K.M. Smith[53], M. Smizanska[71], K. Smolek[127], A.A. Snesarev[94], S.W. Snow[82], J. Snow[111], J. Snuverink[105], S. Snyder[24], M. Soares[124a], R. Sobie[169,j], J. Sodomka[127], A. Soffer[153], C.A. Solans[167], M. Solar[127], J. Solc[127], E. Soldatov[96], U. Soldevila[167], E. Solfaroli Camillocci[132a,132b], A.A. Solodkov[128], O.V. Solovyanov[128], J. Sondericker[24], N. Soni[2], V. Sopko[127], B. Sopko[127], M. Sorbi[89a,89b], M. Sosebee[7], A. Soukharev[107], S. Spagnolo[72a,72b], F. Spanò[34], R. Spighi[19a], G. Spigo[29], F. Spila[132a,132b], E. Spiriti[134a], R. Spiwoks[29], M. Spousta[126], T. Spreitzer[158], B. Spurlock[7], R.D. St. Denis[53], T. Stahl[141], J. Stahlman[120], R. Stamen[58a], E. Stanecka[29], R.W. Stanek[5], C. Stanescu[134a], S. Stapnes[117], E.A. Starchenko[128], J. Stark[55], P. Staroba[125], P. Starovoitov[91], A. Staude[98], P. Stavina[144a], G. Stavropoulos[14], G. Steele[53], P. Steinbach[43], P. Steinberg[24], I. Stekl[127], B. Stelzer[142], H.J. Stelzer[41], O. Stelzer-Chilton[159a], H. Stenzel[52], K. Stevenson[75], G.A. Stewart[29], J.A. Stillings[20], T. Stockmanns[20], M.C. Stockton[29], K. Stoerig[48], G. Stoicea[25a], S. Stonjek[99], P. Strachota[126], A.R. Stradling[7], A. Straessner[43], J. Strandberg[147], S. Strandberg[146a,146b], A. Strandlie[117], M. Strang[109], E. Strauss[143], M. Strauss[111], P. Strizenec[144b], R. Ströhmer[173], D.M. Strom[114], J.A. Strong[76,*], R. Stroynowski[39], J. Strube[129], B. Stugu[13], I. Stumer[24,*], J. Stupak[148], P. Sturm[174], D.A. Soh[151,q], D. Su[143], H.S. Subramania[2], A. Succurro[11], Y. Sugaya[116], T. Sugimoto[101], C. Suhr[106], K. Suita[67], M. Suk[126], V.V. Sulin[94], S. Sultansoy[3d], T. Sumida[29], X. Sun[55], J.E. Sundermann[48], K. Suruliz[139], S. Sushkov[11], G. Susinno[36a,36b], M.R. Sutton[149], Y. Suzuki[66], M. Svatos[125], Yu.M. Sviridov[128], S. Swedish[168], I. Sykora[144a], T. Sykora[126], B. Szeless[29], J. Sánchez[167], D. Ta[105], K. Tackmann[41], A. Taffard[163], R. Tafirout[159a], A. Taga[117], N. Taiblum[153], Y. Takahashi[101], H. Takai[24], R. Takashima[69], H. Takeda[67], T. Takeshita[140], M. Talby[83], A. Talyshev[107], M.C. Tamsett[24], J. Tanaka[155], R. Tanaka[115], S. Tanaka[131], S. Tanaka[66], Y. Tanaka[100], K. Tani[67], N. Tannoury[83], G.P. Tappern[29], S. Tapprogge[81], D. Tardif[158], S. Tarem[152], F. Tarrade[24], G.F. Tartarelli[89a], P. Tas[126], M. Tasevsky[125], E. Tassi[36a,36b], M. Tatarkhanov[14], C. Taylor[77], F.E. Taylor[92], G.N. Taylor[86], W. Taylor[159b], M. Teixeira Dias Castanheira[75], P. Teixeira-Dias[76], K.K. Temming[48], H. Ten Kate[29], P.K. Teng[151], S. Terada[66], K. Terashi[155], J. Terron[80], M. Terwort[41,o], M. Testa[47], R.J. Teuscher[158,j], J. Thadome[174], J. Therhaag[20], T. Theveneaux-Pelzer[78], M. Thioye[175], S. Thoma[48], J.P. Thomas[17], E.N. Thompson[84], P.D. Thompson[17], P.D. Thompson[158], A.S. Thompson[53], E. Thomson[120], M. Thomson[27], R.P. Thun[87], T. Tic[125], V.O. Tikhomirov[94], Y.A. Tikhonov[107], C.J.W.P. Timmermans[104], P. Tipton[175], S. Tisserant[83], J. Tobias[48], B. Toczek[37], T. Todorov[4], S. Todorova-Nova[161], B. Toggerson[163], J. Tojo[66], S. Tokár[144a], K. Tokunaga[67], K. Tokushuku[66], K. Tollefson[88], M. Tomoto[101], L. Tompkins[14], K. Toms[103], G. Tong[32a], A. Tonoyan[13], C. Topfel[16], N.D. Topilin[65], I. Torchiani[29], E. Torrence[114], H. Torres[78], E. Torró Pastor[167], J. Toth[83,x], F. Touchard[83], D.R. Tovey[139], D. Traynor[75], T. Trefzger[173], L. Tremblet[29], A. Tricoli[29], I.M. Trigger[159a], S. Trincaz-Duvoid[78], T.N. Trinh[78], M.F. Tripiana[70], W. Trischuk[158], A. Trivedi[24,w], B. Trocmé[55], C. Troncon[89a], M. Trottier-McDonald[142], A. Trzupek[38], C. Tsarouchas[29], J.C.-L. Tseng[118], M. Tsiakiris[105], P.V. Tsiareshka[90], D. Tsionou[4], G. Tsipolitis[9], V. Tsiskaridze[48], E.G. Tskhadadze[51], I.I. Tsukerman[95], V. Tsulaia[123], J.-W. Tsung[20], S. Tsuno[66], D. Tsybychev[148], A. Tua[139], J.M. Tuggle[30], M. Turala[38], D. Turecek[127], I. Turk Cakir[3e], E. Turlay[105], R. Turra[89a,89b], P.M. Tuts[34], A. Tykhonov[74], M. Tylmad[146a,146b], M. Tyndel[129], H. Tyrvainen[29], G. Tzanakos[8], K. Uchida[20], I. Ueda[155], R. Ueno[28], M. Ugland[13], M. Uhlenbrock[20], M. Uhrmacher[54], F. Ukegawa[160], G. Unal[29], D.G. Underwood[5], A. Undrus[24], G. Unel[163], Y. Unno[66], D. Urbaniec[34], E. Urkovsky[153], P. Urrejola[31a], G. Usai[7], M. Uslenghi[119a,119b], L. Vacavant[83], V. Vacek[127], B. Vachon[85], S. Vahsen[14], J. Valenta[125], P. Valente[132a], S. Valentinetti[19a,19b], S. Valkar[126], E. Valladolid Gallego[167], S. Vallecorsa[152], J.A. Valls Ferrer[167], H. van der Graaf[105], E. van der Kraaij[105], R. Van Der Leeuw[105], E. van der Poel[105], D. van der Ster[29], B. Van Eijk[105], N. van Eldik[84], P. van Gemmeren[5], Z. van Kesteren[105], I. van Vulpen[105], W. Vandelli[29], G. Vandoni[29], A. Vaniachine[5], P. Vankov[41], F. Vannucci[78], F. Varela Rodriguez[29], R. Vari[132a], E.W. Varnes[6], D. Varouchas[14], A. Vartapetian[7], K.E. Varvell[150], V.I. Vassilakopoulos[56], F. Vazeille[33], G. Vegni[89a,89b], J.J. Veillet[115], C. Vellidis[8], F. Veloso[124a], R. Veness[29], S. Veneziano[132a], A. Ventura[72a,72b], D. Ventura[138], M. Venturi[48], N. Venturi[16], V. Vercesi[119a], M. Verducci[138], W. Verkerke[105], J.C. Vermeulen[105], A. Vest[43], M.C. Vetterli[142,e], I. Vichou[165], T. Vickey[145b,z], G.H.A. Viehhauser[118], S. Viel[168], M. Villa[19a,19b], M. Villaplana Perez[167], E. Vilucchi[47], M.G. Vincter[28], E. Vinek[29], V.B. Vinogradov[65], M. Virchaux[136,*], S. Viret[33], J. Virzi[14], A. Vitale[19a,19b], O. Vitells[171], M. Viti[41], I. Vivarelli[48], F. Vives Vaque[11], S. Vlachos[9], M. Vlasak[127], N. Vlasov[20], A. Vogel[20], P. Vokac[127], G. Volpi[47], M. Volpi[11], G. Volpini[89a], H. von der Schmitt[99], J. von Loeben[99], H. von Radziewski[48], E. von Toerne[20], V. Vorobel[126], A.P. Vorobiev[128], V. Vorwerk[11], M. Vos[167], R. Voss[29], T.T. Voss[174], J.H. Vossebeld[73], N. Vranjes[12a], M. Vranjes Milosavljevic[12a], V. Vrba[125], M. Vreeswijk[105], T. Vu Anh[81], R. Vuillermet[29], I. Vukotic[115], W. Wagner[174], P. Wagner[120], H. Wahlen[174], J. Wakabayashi[101], J. Walbersloh[42], S. Walch[87], J. Walder[71], R. Walker[98], W. Walkowiak[141], R. Wall[175], P. Waller[73], C. Wang[44], H. Wang[172], H. Wang[32b,aa], J. Wang[151], J. Wang[32d], J.C. Wang[138], R. Wang[103], S.M. Wang[151], A. Warburton[85], C.P. Ward[27], M. Warsinsky[48], P.M. Watkins[17], A.T. Watson[17], M.F. Watson[17], G. Watts[138], S. Watts[82], A.T. Waugh[150], B.M. Waugh[77], J. Weber[42], M. Weber[129], M.S. Weber[16], P. Weber[54], A.R. Weidberg[118], P. Weigell[99], J. Weingarten[54], C. Weiser[48], H. Wellenstein[22], P.S. Wells[29], M. Wen[47], T. Wenaus[24],

S. Wendler[123], Z. Weng[151,q], T. Wengler[29], S. Wenig[29], N. Wermes[20], M. Werner[48], P. Werner[29], M. Werth[163], M. Wessels[58a], C. Weydert[55], K. Whalen[28], S.J. Wheeler-Ellis[163], S.P. Whitaker[21], A. White[7], M.J. White[86], S. White[24], S.R. Whitehead[118], D. Whiteson[163], D. Whittington[61], F. Wicek[115], D. Wicke[174], F.J. Wickens[129], W. Wiedenmann[172], M. Wielers[129], P. Wienemann[20], C. Wiglesworth[75], L.A.M. Wiik[48], P.A. Wijeratne[77], A. Wildauer[167], M.A. Wildt[41,o], I. Wilhelm[126], H.G. Wilkens[29], J.Z. Will[98], E. Williams[34], H.H. Williams[120], W. Willis[34], S. Willocq[84], J.A. Wilson[17], M.G. Wilson[143], A. Wilson[87], I. Wingerter-Seez[4], S. Winkelmann[48], F. Winklmeier[29], M. Wittgen[143], M.W. Wolter[38], H. Wolters[124a,h], G. Wooden[118], B.K. Wosiek[38], J. Wotschack[29], M.J. Woudstra[84], K. Wraight[53], C. Wright[53], B. Wrona[73], S.L. Wu[172], X. Wu[49], Y. Wu[32b,ab], E. Wulf[34], R. Wunstorf[42], B.M. Wynne[45], L. Xaplanteris[9], S. Xella[35], S. Xie[48], Y. Xie[32a], C. Xu[32b,ac], D. Xu[139], G. Xu[32a], B. Yabsley[150], M. Yamada[66], A. Yamamoto[66], K. Yamamoto[64], S. Yamamoto[155], T. Yamamura[155], J. Yamaoka[44], T. Yamazaki[155], Y. Yamazaki[67], Z. Yan[21], H. Yang[87], U.K. Yang[82], Y. Yang[61], Y. Yang[32a], Z. Yang[146a,146b], S. Yanush[91], W.-M. Yao[14], Y. Yao[14], Y. Yasu[66], G.V. Ybeles Smit[130], J. Ye[39], S. Ye[24], M. Yilmaz[3c], R. Yoosoofmiya[123], K. Yorita[170], R. Yoshida[5], C. Young[143], S. Youssef[21], D. Yu[24], J. Yu[7], J. Yu[32c,ac], L. Yuan[32a,ad], A. Yurkewicz[148], V.G. Zaets[128], R. Zaidan[63], A.M. Zaitsev[128], Z. Zajacova[29], Yo.K. Zalite[121], L. Zanello[132a,132b], P. Zarzhitsky[39], A. Zaytsev[107], C. Zeitnitz[174], M. Zeller[175], A. Zemla[38], C. Zendler[20], A.V. Zenin[128], O. Zenin[128], T. Ženiš[144a], Z. Zenonos[122a,122b], S. Zenz[14], D. Zerwas[115], G. Zevi della Porta[57], Z. Zhan[32d], D. Zhang[32b,aa], H. Zhang[88], J. Zhang[5], X. Zhang[32d], Z. Zhang[115], L. Zhao[108], T. Zhao[138], Z. Zhao[32b], A. Zhemchugov[65], S. Zheng[32a], J. Zhong[151,ae], B. Zhou[87], N. Zhou[163], Y. Zhou[151], C.G. Zhu[32d], H. Zhu[41], Y. Zhu[172], X. Zhuang[98], V. Zhuravlov[99], D. Zieminska[61], R. Zimmermann[20], S. Zimmermann[20], S. Zimmermann[48], M. Ziolkowski[141], R. Zitoun[4], L. Živković[34], V.V. Zmouchko[128,*], G. Zobernig[172], A. Zoccoli[19a,19b], Y. Zolnierowski[4], A. Zsenei[29], M. zur Nedden[15], V. Zutshi[106], L. Zwalinski[29]

[1]University at Albany, Albany NY, United States of America
[2]Department of Physics, University of Alberta, Edmonton AB, Canada
[3(a)]Department of Physics, Ankara University, Ankara; [(b)]Department of Physics, Dumlupinar University, Kutahya; [(c)]Department of Physics, Gazi University, Ankara; [(d)]Division of Physics, TOBB University of Economics and Technology, Ankara; [(e)]Turkish Atomic Energy Authority, Ankara, Turkey
[4]LAPP, CNRS/IN2P3 and Université de Savoie, Annecy-le-Vieux, France
[5]High Energy Physics Division, Argonne National Laboratory, Argonne IL, United States of America
[6]Department of Physics, University of Arizona, Tucson AZ, United States of America
[7]Department of Physics, The University of Texas at Arlington, Arlington TX, United States of America
[8]Physics Department, University of Athens, Athens, Greece
[9]Physics Department, National Technical University of Athens, Zografou, Greece
[10]Institute of Physics, Azerbaijan Academy of Sciences, Baku, Azerbaijan
[11]Institut de Física d'Altes Energies and Universitat Autònoma de Barcelona and ICREA, Barcelona, Spain
[12(a)]Institute of Physics, University of Belgrade, Belgrade; [(b)]Vinca Institute of Nuclear Sciences, Belgrade, Serbia
[13]Department for Physics and Technology, University of Bergen, Bergen, Norway
[14]Physics Division, Lawrence Berkeley National Laboratory and University of California, Berkeley CA, United States of America
[15]Department of Physics, Humboldt University, Berlin, Germany
[16]Albert Einstein Center for Fundamental Physics and Laboratory for High Energy Physics, University of Bern, Bern, Switzerland
[17]School of Physics and Astronomy, University of Birmingham, Birmingham, United Kingdom
[18(a)]Department of Physics, Bogazici University, Istanbul; [(b)]Division of Physics, Dogus University, Istanbul; [(c)]Department of Physics Engineering, Gaziantep University, Gaziantep; [(d)]Department of Physics, Istanbul Technical University, Istanbul, Turkey
[19(a)]INFN Sezione di Bologna; [(b)]Dipartimento di Fisica, Università di Bologna, Bologna, Italy
[20]Physikalisches Institut, University of Bonn, Bonn, Germany
[21]Department of Physics, Boston University, Boston MA, United States of America
[22]Department of Physics, Brandeis University, Waltham MA, United States of America
[23(a)]Universidade Federal do Rio De Janeiro COPPE/EE/IF, Rio de Janeiro; [(b)]Instituto de Fisica, Universidade de Sao Paulo, Sao Paulo, Brazil
[24]Physics Department, Brookhaven National Laboratory, Upton NY, United States of America
[25(a)]National Institute of Physics and Nuclear Engineering, Bucharest; [(b)]University Politehnica Bucharest, Bucharest; [(c)]West University in Timisoara, Timisoara, Romania
[26]Departamento de Física, Universidad de Buenos Aires, Buenos Aires, Argentina

[27]Cavendish Laboratory, University of Cambridge, Cambridge, United Kingdom
[28]Department of Physics, Carleton University, Ottawa ON, Canada
[29]CERN, Geneva, Switzerland
[30]Enrico Fermi Institute, University of Chicago, Chicago IL, United States of America
[31][(a)]Departamento de Fisica, Pontificia Universidad Católica de Chile, Santiago; [(b)]Departamento de Física, Universidad Técnica Federico Santa María, Valparaíso, Chile
[32][(a)]Institute of High Energy Physics, Chinese Academy of Sciences, Beijing; [(b)]Department of Modern Physics, University of Science and Technology of China, Anhui; [(c)]Department of Physics, Nanjing University, Jiangsu; [(d)]High Energy Physics Group, Shandong University, Shandong, China
[33]Laboratoire de Physique Corpusculaire, Clermont Université and Université Blaise Pascal and CNRS/IN2P3, Aubiere Cedex, France
[34]Nevis Laboratory, Columbia University, Irvington NY, United States of America
[35]Niels Bohr Institute, University of Copenhagen, Kobenhavn, Denmark
[36][(a)]INFN Gruppo Collegato di Cosenza; [(b)]Dipartimento di Fisica, Università della Calabria, Arcavata di Rende, Italy
[37]Faculty of Physics and Applied Computer Science, AGH-University of Science and Technology, Krakow, Poland
[38]The Henryk Niewodniczanski Institute of Nuclear Physics, Polish Academy of Sciences, Krakow, Poland
[39]Physics Department, Southern Methodist University, Dallas TX, United States of America
[40]Physics Department, University of Texas at Dallas, Richardson TX, United States of America
[41]DESY, Hamburg and Zeuthen, Germany
[42]Institut für Experimentelle Physik IV, Technische Universität Dortmund, Dortmund, Germany
[43]Institut für Kern- und Teilchenphysik, Technical University Dresden, Dresden, Germany
[44]Department of Physics, Duke University, Durham NC, United States of America
[45]SUPA – School of Physics and Astronomy, University of Edinburgh, Edinburgh, United Kingdom
[46]Fachhochschule Wiener Neustadt, Johannes Gutenbergstrasse 3, 2700 Wiener Neustadt, Austria
[47]INFN Laboratori Nazionali di Frascati, Frascati, Italy
[48]Fakultät für Mathematik und Physik, Albert-Ludwigs-Universität, Freiburg i.Br., Germany
[49]Section de Physique, Université de Genève, Geneva, Switzerland
[50][(a)]INFN Sezione di Genova; [(b)]Dipartimento di Fisica, Università di Genova, Genova, Italy
[51]Institute of Physics and HEP Institute, Georgian Academy of Sciences and Tbilisi State University, Tbilisi, Georgia
[52]II Physikalisches Institut, Justus-Liebig-Universität Giessen, Giessen, Germany
[53]SUPA – School of Physics and Astronomy, University of Glasgow, Glasgow, United Kingdom
[54]II Physikalisches Institut, Georg-August-Universität, Göttingen, Germany
[55]Laboratoire de Physique Subatomique et de Cosmologie, Université Joseph Fourier and CNRS/IN2P3 and Institut National Polytechnique de Grenoble, Grenoble, France
[56]Department of Physics, Hampton University, Hampton VA, United States of America
[57]Laboratory for Particle Physics and Cosmology, Harvard University, Cambridge MA, United States of America
[58][(a)]Kirchhoff-Institut für Physik, Ruprecht-Karls-Universität Heidelberg, Heidelberg; [(b)]Physikalisches Institut, Ruprecht-Karls-Universität Heidelberg, Heidelberg; [(c)]ZITI Institut für technische Informatik, Ruprecht-Karls-Universität Heidelberg, Mannheim, Germany
[59]Faculty of Science, Hiroshima University, Hiroshima, Japan
[60]Faculty of Applied Information Science, Hiroshima Institute of Technology, Hiroshima, Japan
[61]Department of Physics, Indiana University, Bloomington IN, United States of America
[62]Institut für Astro- und Teilchenphysik, Leopold-Franzens-Universität, Innsbruck, Austria
[63]University of Iowa, Iowa City IA, United States of America
[64]Department of Physics and Astronomy, Iowa State University, Ames IA, United States of America
[65]Joint Institute for Nuclear Research, JINR Dubna, Dubna, Russia
[66]KEK, High Energy Accelerator Research Organization, Tsukuba, Japan
[67]Graduate School of Science, Kobe University, Kobe, Japan
[68]Faculty of Science, Kyoto University, Kyoto, Japan
[69]Kyoto University of Education, Kyoto, Japan
[70]Instituto de Física La Plata, Universidad Nacional de La Plata and CONICET, La Plata, Argentina
[71]Physics Department, Lancaster University, Lancaster, United Kingdom
[72][(a)]INFN Sezione di Lecce; [(b)]Dipartimento di Fisica, Università del Salento, Lecce, Italy

[73]Oliver Lodge Laboratory, University of Liverpool, Liverpool, United Kingdom
[74]Department of Physics, Jožef Stefan Institute and University of Ljubljana, Ljubljana, Slovenia
[75]Department of Physics, Queen Mary University of London, London, United Kingdom
[76]Department of Physics, Royal Holloway University of London, Surrey, United Kingdom
[77]Department of Physics and Astronomy, University College London, London, United Kingdom
[78]Laboratoire de Physique Nucléaire et de Hautes Energies, UPMC and Université Paris-Diderot and CNRS/IN2P3, Paris, France
[79]Fysiska institutionen, Lunds universitet, Lund, Sweden
[80]Departamento de Fisica Teorica C-15, Universidad Autonoma de Madrid, Madrid, Spain
[81]Institut für Physik, Universität Mainz, Mainz, Germany
[82]School of Physics and Astronomy, University of Manchester, Manchester, United Kingdom
[83]CPPM, Aix-Marseille Université and CNRS/IN2P3, Marseille, France
[84]Department of Physics, University of Massachusetts, Amherst MA, United States of America
[85]Department of Physics, McGill University, Montreal QC, Canada
[86]School of Physics, University of Melbourne, Victoria, Australia
[87]Department of Physics, The University of Michigan, Ann Arbor MI, United States of America
[88]Department of Physics and Astronomy, Michigan State University, East Lansing MI, United States of America
[89(a)]INFN Sezione di Milano; [(b)]Dipartimento di Fisica, Università di Milano, Milano, Italy
[90]B.I. Stepanov Institute of Physics, National Academy of Sciences of Belarus, Minsk, Republic of Belarus
[91]National Scientific and Educational Centre for Particle and High Energy Physics, Minsk, Republic of Belarus
[92]Department of Physics, Massachusetts Institute of Technology, Cambridge MA, United States of America
[93]Group of Particle Physics, University of Montreal, Montreal QC, Canada
[94]P.N. Lebedev Institute of Physics, Academy of Sciences, Moscow, Russia
[95]Institute for Theoretical and Experimental Physics (ITEP), Moscow, Russia
[96]Moscow Engineering and Physics Institute (MEPhI), Moscow, Russia
[97]Skobeltsyn Institute of Nuclear Physics, Lomonosov Moscow State University, Moscow, Russia
[98]Fakultät für Physik, Ludwig-Maximilians-Universität München, München, Germany
[99]Max-Planck-Institut für Physik (Werner-Heisenberg-Institut), München, Germany
[100]Nagasaki Institute of Applied Science, Nagasaki, Japan
[101]Graduate School of Science, Nagoya University, Nagoya, Japan
[102(a)]INFN Sezione di Napoli; [(b)]Dipartimento di Scienze Fisiche, Università di Napoli, Napoli, Italy
[103]Department of Physics and Astronomy, University of New Mexico, Albuquerque NM, United States of America
[104]Institute for Mathematics, Astrophysics and Particle Physics, Radboud University Nijmegen/Nikhef, Nijmegen, Netherlands
[105]Nikhef National Institute for Subatomic Physics and University of Amsterdam, Amsterdam, Netherlands
[106]Department of Physics, Northern Illinois University, DeKalb IL, United States of America
[107]Budker Institute of Nuclear Physics (BINP), Novosibirsk, Russia
[108]Department of Physics, New York University, New York NY, United States of America
[109]Ohio State University, Columbus OH, United States of America
[110]Faculty of Science, Okayama University, Okayama, Japan
[111]Homer L. Dodge Department of Physics and Astronomy, University of Oklahoma, Norman OK, United States of America
[112]Department of Physics, Oklahoma State University, Stillwater OK, United States of America
[113]Palacký University, RCPTM, Olomouc, Czech Republic
[114]Center for High Energy Physics, University of Oregon, Eugene OR, United States of America
[115]LAL, Univ. Paris-Sud and CNRS/IN2P3, Orsay, France
[116]Graduate School of Science, Osaka University, Osaka, Japan
[117]Department of Physics, University of Oslo, Oslo, Norway
[118]Department of Physics, Oxford University, Oxford, United Kingdom
[119(a)]INFN Sezione di Pavia; [(b)]Dipartimento di Fisica Nucleare e Teorica, Università di Pavia, Pavia, Italy
[120]Department of Physics, University of Pennsylvania, Philadelphia PA, United States of America
[121]Petersburg Nuclear Physics Institute, Gatchina, Russia
[122(a)]INFN Sezione di Pisa; [(b)]Dipartimento di Fisica E. Fermi, Università di Pisa, Pisa, Italy

[123]Department of Physics and Astronomy, University of Pittsburgh, Pittsburgh PA, United States of America
[124(a)]Laboratorio de Instrumentacao e Fisica Experimental de Particulas – LIP, Lisboa, Portugal; [(b)]Departamento de Fisica Teorica y del Cosmos and CAFPE, Universidad de Granada, Granada, Spain
[125]Institute of Physics, Academy of Sciences of the Czech Republic, Praha, Czech Republic
[126]Faculty of Mathematics and Physics, Charles University in Prague, Praha, Czech Republic
[127]Czech Technical University in Prague, Praha, Czech Republic
[128]State Research Center Institute for High Energy Physics, Protvino, Russia
[129]Particle Physics Department, Rutherford Appleton Laboratory, Didcot, United Kingdom
[130]Physics Department, University of Regina, Regina SK, Canada
[131]Ritsumeikan University, Kusatsu, Shiga, Japan
[132(a)]INFN Sezione di Roma I; [(b)]Dipartimento di Fisica, Università La Sapienza, Roma, Italy
[133(a)]INFN Sezione di Roma Tor Vergata; [(b)]Dipartimento di Fisica, Università di Roma Tor Vergata, Roma, Italy
[134(a)]INFN Sezione di Roma Tre; [(b)]Dipartimento di Fisica, Università Roma Tre, Roma, Italy
[135(a)]Faculté des Sciences Ain Chock, Réseau Universitaire de Physique des Hautes Energies – Université Hassan II, Casablanca; [(b)]Centre National de l'Energie des Sciences Techniques Nucleaires, Rabat; [(c)]Faculté des Sciences Semlalia Département de Physique, Université Cadi Ayyad, B.P. 2390 Marrakech 40000; [(d)]Faculté des Sciences, Université Mohamed Premier and LPTPM, Oujda; [(e)]Faculté des Sciences, Université Mohammed V, Rabat, Morocco
[136]DSM/IRFU (Institut de Recherches sur les Lois Fondamentales de l'Univers), CEA Saclay (Commissariat a l'Energie Atomique), Gif-sur-Yvette, France
[137]Santa Cruz Institute for Particle Physics, University of California Santa Cruz, Santa Cruz CA, United States of America
[138]Department of Physics, University of Washington, Seattle WA, United States of America
[139]Department of Physics and Astronomy, University of Sheffield, Sheffield, United Kingdom
[140]Department of Physics, Shinshu University, Nagano, Japan
[141]Fachbereich Physik, Universität Siegen, Siegen, Germany
[142]Department of Physics, Simon Fraser University, Burnaby BC, Canada
[143]SLAC National Accelerator Laboratory, Stanford CA, United States of America
[144(a)]Faculty of Mathematics, Physics & Informatics, Comenius University, Bratislava; [(b)]Department of Subnuclear Physics, Institute of Experimental Physics of the Slovak Academy of Sciences, Kosice, Slovak Republic
[145(a)]Department of Physics, University of Johannesburg; [(b)]School of Physics, University of the Witwatersrand, Johannesburg, South Africa
[146(a)]Department of Physics, Stockholm University; [(b)]The Oskar Klein Centre, Stockholm, Sweden
[147]Physics Department, Royal Institute of Technology, Stockholm, Sweden
[148]Department of Physics and Astronomy, Stony Brook University, Stony Brook NY, United States of America
[149]Department of Physics and Astronomy, University of Sussex, Brighton, United Kingdom
[150]School of Physics, University of Sydney, Sydney, Australia
[151]Institute of Physics, Academia Sinica, Taipei, Taiwan
[152]Department of Physics, Technion: Israel Inst. of Technology, Haifa, Israel
[153]Raymond and Beverly Sackler School of Physics and Astronomy, Tel Aviv University, Tel Aviv, Israel
[154]Department of Physics, Aristotle University of Thessaloniki, Thessaloniki, Greece
[155]International Center for Elementary Particle Physics and Department of Physics, The University of Tokyo, Tokyo, Japan
[156]Graduate School of Science and Technology, Tokyo Metropolitan University, Tokyo, Japan
[157]Department of Physics, Tokyo Institute of Technology, Tokyo, Japan
[158]Department of Physics, University of Toronto, Toronto ON, Canada
[159(a)]TRIUMF, Vancouver BC; [(b)]Department of Physics and Astronomy, York University, Toronto ON, Canada
[160]Institute of Pure and Applied Sciences, University of Tsukuba, Ibaraki, Japan
[161]Science and Technology Center, Tufts University, Medford MA, United States of America
[162]Centro de Investigaciones, Universidad Antonio Narino, Bogota, Colombia
[163]Department of Physics and Astronomy, University of California Irvine, Irvine CA, United States of America
[164(a)]INFN Gruppo Collegato di Udine, Udine; [(b)]ICTP, Trieste; [(c)]Dipartimento di Fisica, Università di Udine, Udine, Italy
[165]Department of Physics, University of Illinois, Urbana IL, United States of America
[166]Department of Physics and Astronomy, University of Uppsala, Uppsala, Sweden
[167]Instituto de Física Corpuscular (IFIC) and Departamento de Física Atómica, Molecular y Nuclear and Departamento de Ingenierá Electrónica and Instituto de Microelectrónica de Barcelona (IMB-CNM), University of Valencia and CSIC, Valencia, Spain

[168]Department of Physics, University of British Columbia, Vancouver BC, Canada
[169]Department of Physics and Astronomy, University of Victoria, Victoria BC, Canada
[170]Waseda University, Tokyo, Japan
[171]Department of Particle Physics, The Weizmann Institute of Science, Rehovot, Israel
[172]Department of Physics, University of Wisconsin, Madison WI, United States of America
[173]Fakultät für Physik und Astronomie, Julius-Maximilians-Universität, Würzburg, Germany
[174]Fachbereich C Physik, Bergische Universität Wuppertal, Wuppertal, Germany
[175]Department of Physics, Yale University, New Haven CT, United States of America
[176]Yerevan Physics Institute, Yerevan, Armenia
[177]Domaine scientifique de la Doua, Centre de Calcul CNRS/IN2P3, Villeurbanne Cedex, France
[a]Also at Laboratorio de Instrumentacao e Fisica Experimental de Particulas – LIP, Lisboa, Portugal
[b]Also at Faculdade de Ciencias and CFNUL, Universidade de Lisboa, Lisboa, Portugal
[c]Also at Particle Physics Department, Rutherford Appleton Laboratory, Didcot, United Kingdom
[d]Also at CPPM, Aix-Marseille Université and CNRS/IN2P3, Marseille, France
[e]Also at TRIUMF, Vancouver BC, Canada
[f]Also at Department of Physics, California State University, Fresno CA, United States of America
[g]Also at Faculty of Physics and Applied Computer Science, AGH-University of Science and Technology, Krakow, Poland
[h]Also at Department of Physics, University of Coimbra, Coimbra, Portugal
[i]Also at Università di Napoli Parthenope, Napoli, Italy
[j]Also at Institute of Particle Physics (IPP), Canada
[k]Also at Department of Physics, Middle East Technical University, Ankara, Turkey
[l]Also at Louisiana Tech University, Ruston LA, United States of America
[m]Also at Group of Particle Physics, University of Montreal, Montreal QC, Canada
[n]Also at Institute of Physics, Azerbaijan Academy of Sciences, Baku, Azerbaijan
[o]Also at Institut für Experimentalphysik, Universität Hamburg, Hamburg, Germany
[p]Also at Manhattan College, New York NY, United States of America
[q]Also at School of Physics and Engineering, Sun Yat-sen University, Guanzhou, China
[r]Also at Academia Sinica Grid Computing, Institute of Physics, Academia Sinica, Taipei, Taiwan
[s]Also at High Energy Physics Group, Shandong University, Shandong, China
[t]Also at California Institute of Technology, Pasadena CA, United States of America
[u]Also at Section de Physique, Université de Genève, Geneva, Switzerland
[v]Also at Departamento de Fisica, Universidade de Minho, Braga, Portugal
[w]Also at Department of Physics and Astronomy, University of South Carolina, Columbia SC, United States of America
[x]Also at KFKI Research Institute for Particle and Nuclear Physics, Budapest, Hungary
[y]Also at Institute of Physics, Jagiellonian University, Krakow, Poland
[z]Also at Department of Physics, Oxford University, Oxford, United Kingdom
[aa]Also at Institute of Physics, Academia Sinica, Taipei, Taiwan
[ab]Also at Department of Physics, The University of Michigan, Ann Arbor MI, United States of America
[ac]Also at DSM/IRFU (Institut de Recherches sur les Lois Fondamentales de l'Univers), CEA Saclay (Commissariat a l'Energie Atomique), Gif-sur-Yvette, France
[ad]Also at Laboratoire de Physique Nucléaire et de Hautes Energies, UPMC and Université Paris-Diderot and CNRS/IN2P3, Paris, France
[ae]Also at Department of Physics, Nanjing University, Jiangsu, China
[*]Deceased